# Seabirds in 3D: A Framework to Evaluate Collision Vulnerability with Future Offshore Wind Developments

**Interim Project Report #2:** Assessing Tradeoffs between Seabird Density at Collision Risk Height and Wind Facility Performance

This report was prepared by the Schatz Energy Research Center and H. T. Harvey & Associates for the California Energy Commission and published in April 2025.

**Disclaimer**

This project was funded by the California Energy Commission. The content does not represent the official views of policies of the State of California. This report was created under agreement number: EPC-19-011

**About the Schatz Energy Research Center**

The Schatz Energy Research Center at Cal Poly Humboldt advances clean and renewable energy. Our projects aim to reduce climate change and pollution while increasing energy access and resilience. Our work is collaborative and multidisciplinary, and we are grateful to the many partners who together make our efforts possible. Learn more about our work at schatzcenter.org

**About H. T. Harvey & Associates**

H. T. Harvey & Associates is an ecological consulting firm whose mission is to create ecologically sound solutions to complex natural resource challenges. We apply our expertise in wildlife ecology, aquatic ecology, plant ecology, restoration ecology, and landscape architecture in pursuit of this mission and we have delivered exceptional consulting services to public agencies, private entities, and nonprofit organizations since 1970. Our staff expertise encompasses a wide range of biological and design disciplines (wildlife ecology, aquatic ecology, plant ecology, restoration ecology, and landscape architecture).

**Rights and Permissions**



Wallach, Eli., Charles Chamberlin, Stephanie Schneider, Sophie Bernstein, Sadie Trush, Sharon Kramer, Scott Terrill, David Ainley, Arne Jacobson (2025). Seabirds in 3D: A Framework to Evaluate Collision Vulnerability with Future Offshore Wind Developments. Interim Project Report #2: Assessing Tradeoffs between Seabird Density at Collision Risk Height and Wind Facility Performance Humboldt, CA: Schatz Energy Research Center.



Prepared by the Schatz Energy Research Center and H. T. Harvey & Associates for the California Energy Commission and published by the Schatz Energy Research Center: Humboldt, CA. schatzcenter.org/publications.

## 1. Executive Summary

Herein we assess, using a multi-objective Pareto optimality the degree to which seabirds off the coast of California may collide with turbine rotors under different offshore wind development scenarios relative to wind facility performance. This Multi-objective Pareto Optimality approach is used to analyze trade-offs between seabird densities predicted to be at risk from turbine collisions, as determined by a 3D Seabird Collision Vulnerability Framework (i.e., “3D Framework”), and simulated power generation profiles. This current assessment encompasses all offshore areas between Point Conception, California to Yaquina Head, Oregon, that are shallow enough to support state-of-the-art turbine mooring technologies (e.g., sea floor is within 1,300 m distance from the sea surface). Results presented herein are focused on the outcome for four different seabird groupings: All Modeled Bird Species, California Species of Special Concern (CSSC), Seabirds Listed at the State and/or Federal level (SFTE), and the Black-Footed Albatross.

The 3D Framework predicts that seabird activity is primarily concentrated below rotor swept altitudes, with an average of fewer than 10% of the offshore seabird community predicted to occupy altitudes exceeding 10 meters [m] which is well below the lower extent of rotor swept altitudes at 30 m. Thus, only a small portion of the seabird community is predicted to be present at altitudes of 10 m or greater relative to the sea-surface across the entire region; the average portion of seabird density predicted to be above 10 m vs overall was only 8% across all seabirds included in the 3D Framework, 0.2% for all CSSC seabirds, 0.1% for all SFTE seabirds, and 5.7% for the Black-footed Albatross. Although the overall percentage of birds flying above 10m was 8%, dynamic soaring species and gull are taxonomically disproportionately vulnerable based on their morphology and behavior. However, two endangered species, the short-tailed albatross and the Hawaiian petrel that are dynamic soaring species were too scarce in the study area during the data collection period to provide an adequate sample size to be included in this analysis. The other threatened species with adequate sample sizes comprise murrelets that do not fly above 10 m at sea (aside from marbled murrelets that fly from nearshore coastal waters inland to nest).

The Pareto optimality analysis comparing locations across the study area shows that the two objectives are not very conflicting.  since the best wind resources typically fall further offshore while seabirds tend to be more concentrated near shore. The near-shore estimates of seabird density are strongly affected by the central-place foraging of species breeding locally in coastal habitats, such as cormorants, and western gulls. These combined trends result in convex Pareto fronts showing that these variables are not strongly conflicting (Figures 7-10; top right panes).

When comparing 600MW (fixed build-out size) wind facilities at a variety of proposed wind energy areas and notional areas, northern locations (Crescent City, Cape Mendocino and Humboldt) stood out for falling on or near the Pareto front derived for all of the considered bird species groupings. Additive metrics were used to compare “full buildout” scenarios for the same locations. This analysis shows that increasing wind facility size (turbine count) increases both the annual energy generation and the size of the farm, and thus also the vulnerability of birds to collision. Ideally to compare these different sized wind facilities, flight paths and passage rates would be accounted for. However, due to data limitations, this type of analysis was not possible in the context of the present study.

## 2. Table of Contents

## 3. Project Background

As renewable energy generation in California moves towards a 100% clean energy goal by 2045, as set by Senate Bill (SB) 100, offshore wind has great potential to become an important part of the state's energy profile. As renewable generation increases through the 2020s and 2030s, a diversified set of generation sources will be needed to help manage the balance between generation and load. Offshore of the California coast, persistent strong winds over the ocean are ideal for offshore wind technologies. These technologies have promise to contribute to the state's SB 100 goals. A favorable seasonal and diurnal electricity generation profile highlights the potential for offshore wind to become a cost-competitive energy generation source (Collier et al., 2019; Severy, 2019).

Permitting for offshore wind facilities along the U.S. West Coast will be complicated. One of the many challenges is understanding the potential risk to avian life. While there is some understanding of general hotspots, estimates exist of vulnerability and collision risk within the California Current System (Adams et al., 2017), existing data do not take into account the vertical height dimension. This project estimates the density of seabirds likely present at collision risk height (i.e., within the rotor swept zone), as a function of wind strength, and informs public agency assessments of potential impacts of offshore wind to birds, some of which are of special conservation status. If offshore wind is to help California reach its SB 100 goals, environmental concerns related to potential impacts, including the vulnerability of seabirds to collision, will be an important hurdle to overcome.

This project seeks to advance the understanding of the potential for seabird collisions with offshore wind energy infrastructure off the U.S. West Coast, particularly in waters over the Outer Continental Shelf and slope (OCS) off California, where the ocean windscape and the seabird community differ significantly from nearshore waters along the US/Canadian East Coast and Europe, where most offshore wind generation facilities are located. This goal has been accomplished by combining long-term, at-sea data sets to estimate seabird densities in a way that incorporates the vertical dimension to predict the proportion of the seabird community moving about at heights sufficient to overlap with rotor swept zones.

From these seabird occurrence data, this project devised a 3D Seabird Vulnerability Model that quantifies seabird use of the study area as affected by wind. Results shows seabird hotspots, already identified to some extent by Nur et al. (2011), in terms of 2D species composition and distribution but view them as a function of height, as affected by wind conditions. As a function of morphology and flight behavior, different seabird species use wind to minimize the cost of transport as they travel in search of food. A seabird species' energy balance and use of wind is determined by its morphology, leading some species to fly higher than others, which potentially impacts vulnerability to colliding with offshore turbine rotors. Currently unknown is the degree to which OCS species that fly at RSZ heights might avoid the presence of floating offshore turbines, either at a facility scale (macro-avoidance), row of turbine scale (meso-avoidance) or the scale of a single turbine (micro-avoidance).

To accomplish this comparison between wind energy generation and seabird density, several different wind facility scenarios were investigated in detail along within the study area. Power generation estimates were made leveraging and modifying an Offshore Wind Power Generation Model previously developed (Severy et al., 2020). The Offshore Wind Power Generation Model and 3D Seabird Vulnerability Model were combined and compared using a multi-objective optimization to evaluate possible relationships between seabird density at risk height and wind facility cumulative energy generation potential. Project results allow stakeholders to simultaneously assess site-specific vulnerability of seabird species groups along with wind power generation capacity.

## 4. DESCRIPTION OF TASK 5

The goal of this optimization task was to compare seabird vulnerability to collision with wind facility energy generation. For this task a Pareto optimality approach was selected. Multi-objective optimization was carried out without weighting the two objectives. This Pareto optimality approach was applied to a set of scenarios in which a single turbine is simulated as well as a variety of scenarios considering wind facilities of various capacities at selected locations.

## 5. PRECURSOR ANALYSES

This section briefly describes the two analyses that serve as inputs to the pareto optimality assessment covered in this report. These precursor analyses estimate seabird density at risk height and wind facility power generation. While some detail on the methods used for each is presented below, more complete documentation is available in the Task 3: Seabird Vulnerability and Task 4: Offshore Wind Power Generation Reports.

### 5.1. Seabird Density Estimation

The 3D Framework integrates various analyses to predict the composition and density of California's seabird community. It was applied to 44 most abundant bird species, providing spatially explicit estimates of the seasonal average seabird density above 10m. Annual estimates are also assembled based on a duration-weighted average of seasonal estimates.

Estimation of average seabird density above 10m is best conceptualized as a multi-component analysis, described in detail in the Task 3 report (Schneider et al. 2024) and is summarized here:

● Component I: Relate Flight Heights to Wind Speed

> Seabird species composing California's diverse seabird community were divided into distinct, morphologically-driven Flight Groups (FGs) following Ainley et al. (2015). FG-specific probability curves, indicating the chance of flying above 10m, were generated through mixed-effects logistic regression. For which, an extensive seabird flight behavior dataset was tailored to CCS seabirds across the full spectrum of windspeeds.

● Component II: Predict Densities in 2D

> The year was divided into three oceanographic seasons, which have distinct wind-driven upwelling and temperature regimes (i.e., Upwelling, Oceanic, and Davidson Current). 2D density predictions were made for a 5 minute by 5 minute grid covering the study area, for each species and season.

● Component III: Convert Densities to 3D

> Using outcomes of Components I and II, the dimensionality of density predictions was increased to create a 3D representation of the seabird community. This required a the following steps: (S1) for each location with a 2D density prediction, a distributional representation of the windscape (including extremes) was generated for each season; (S2) this gridded summation of the

windscape was then integrated with the outcome of Component I to derive seasonal-, site-, and FG-specific probabilities of being at collision risk height (Defined as being above 10m above sea level); and (S3) probabilities from S2 were then applied to the outcome of Component II to vertically partition overall density estimates and isolate the seabird density at collision risk height.

The resulting spatially explicit 2D and 3D density predictions were aggregated across seasons and species then visualized using GIS mapping as part of the Task 3 report. This Optimization task report focuses on groups of seabirds rather than individual species, For species-specific density results please reference the Task 3 report.

These 2D and 3D seabird density predictions were based on an Inverse Distance Weighted (IDW) spatial interpolation algorithm, which essentially averages the underlying data. Predictions from the 3D Framework then can be interpreted as the number of birds expected to be present at any given time at the estimated location given the long-term (multi-decadal) conditions observed in the region.

### 5.2. Power Generation and Wind Facility Scenarios

The methods detail by Wallach et al. (2021a,b) were used to estimate the performance of a wind turbine located at the centroid of each of the 5' x 5' cells and of each of the selected wind facility locations and build-outs. In summary, the average annual energy production was estimated for each specific cell location and each specific wind facility location and build-out scenario based on a 20-year time series of modeled wind speeds spanning 1/1/2000 through 12/31/2019, obtained from NREL. NREL-developed power curve models were applied for 12 MW and 15 MW wind turbines. Adjustments were made for power losses due to wake effects (not included in single turbine scenarios), efficiency, availability, and other factors.

Table 1 presents each of the 32 simulated wind facility location and build-out scenarios. The scenarios are defined for 9 locations that include BOEM-defined Wind Energy Areas (WEA), several hypothetical call areas, and other areas of interest. Build-out scenarios for each area include both 12 MW and 15 MW turbine arrays, sized to either fully build-out the available area or create a 600 MW wind facility or in two cases follow a plan proposed by developers. Figure 1 shows the areas studied.

Included in the study areas were the BOEM-Defined wind energy areas (WEA), Humboldt and Morro Bay call areas, leased to wind energy developers in 2022. Also included was the Diablo Canyon WEA, which is no longer being considered by BOEM. In addition to these WEAs, analysis was completed for two notional call areas, one off the coast of Crescent City (Pacific Ocean Energy Trust 2021) and the other off Cape Mendocino. The lease areas proposed off shore of the Vandenberg Air Force Base were also analyzed; Cierco’s CADEMO project and Ideol USA’s Vandenberg Air Force Pilot Project (California State Lands Commission, 2021). Ideol’s Vandenberg project has since been canceled (TGS 2024) though, like the Diablo site, is still included in this analysis.

Modeling was also implemented for areas having historically high levels of bird activity, thus to develop potential book-end tradeoffs among modeled scenarios: Delgada Canyon and the Monterey System. There is no expectation that a windfarm would be developed at these locations, in part (other than seabird density) because. the sea floor in the canyons would be too steep to moor floating turbines.

**Table 1: Wind-facility scenarios simulated to estimate annual power production, which served as the basis for the wind energy performance metric of the Multi-objective Pareto Optimization analysis. The power production estimates from these scenarios were compared against paired seabird vulnerability metrics generated at each Reference Area. Full build-out capacities for each location are provided elsewhere (Table 3, 4).**

| Location | Turbine Specification | Layout | Sizing |
|---|---|---|---|
| Crescent City (Del Norte) | 12 MW | 7D x 10D | Full Build-out |
| Crescent City (Del Norte) | 15 MW | 7D x 10D | Full Build-out |
| Crescent City (Del Norte) | 12 MW | 7D x 10D | 600 MW |
| Crescent City (Del Norte) | 15 MW | 7D x 10D | 600 MW |
| Humboldt | 12 MW | 7D x 10D | Full Build-out |
| Humboldt | 15 MW | 7D x 10D | Full Build-out |
| Humboldt | 12 MW | 7D x 10D | 600 MW |
| Humboldt | 15 MW | 7D x 10D | 600 MW |
| Cape Mendocino | 12 MW | 7D x 10D | Full Build-out |
| Cape Mendocino | 15 MW | 7D x 10D | Full Build-out |
| Cape Mendocino | 12 MW | 7D x 10D | 600 MW |
| Cape Mendocino | 15 MW | 7D x 10D | 600 MW |
| Delgada Canyon | 12 MW | 7D x 10D | 600 MW |
| Delgada Canyon | 15 MW | 7D x 10D | 600 MW |
| Monterey System | 12 MW | 7D x 10D | 600 MW |
| Monterey System | 15 MW | 7D x 10D | 600 MW |
| Morro Bay 376 | 12 MW | 7D x 10D | Full Build-out |
| Morro Bay 376 | 15 MW | 7D x 10D | Full Build-out |
| Morro Bay 376 | 12 MW | 7D x 10D | 600 MW |
| Morro Bay 376 | 15 MW | 7D x 10D | 600 MW |
| Diablo Canyon | 12 MW | 7D x 10D | Full Build-out |
| Diablo Canyon | 15 MW | 7D x 10D | Full Build-out |
| Diablo Canyon | 12 MW | 7D x 10D | 600 MW |
| Diablo Canyon | 15 MW | 7D x 10D | 600 MW |
| CADEMO | 12 MW | As Proposed[i] | 4 Turbines |
| CADEMO | 15 MW | As Proposed[i] | 4 Turbines |
| CADEMO | 12 MW | 7D x 10D | 600 MW |
| CADEMO | 15 MW | 7D x 10D | 600 MW |
| Vandenberg Space Force Base Project | 12 MW | As Proposed[i] | 4 Turbines |
| Vandenberg Space Force Base Project | 15 MW | As Proposed[i] | 4 Turbines |
| Vandenberg Space Force Base Project | 12 MW | 7D x 10D | 600 MW |
| Vandenberg Space Force Base Project | 15 MW | 7D x 10D | 600 MW |

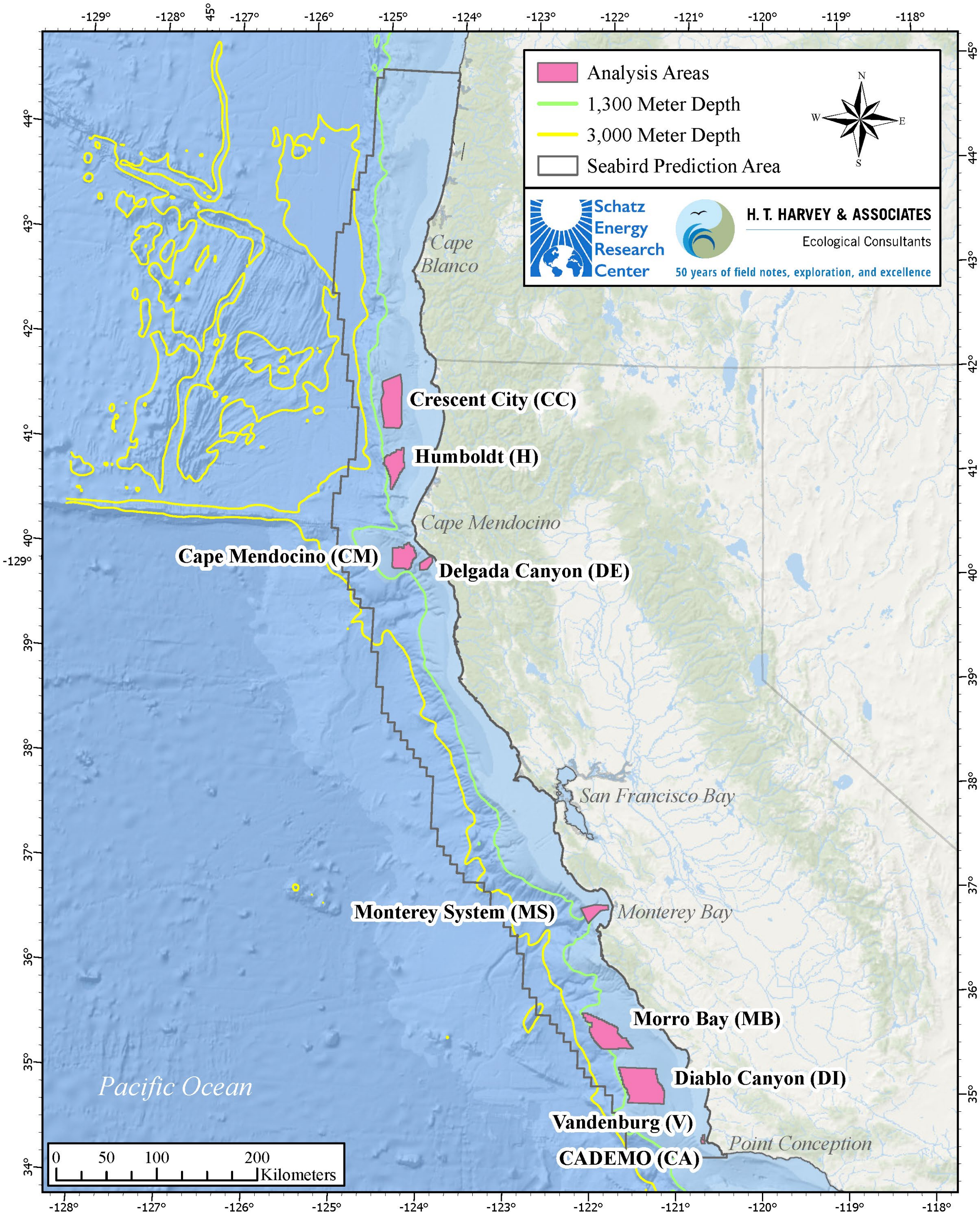


**Figure 1: Map showing the reference areas, the 1300m and 3000m depth contours, and the seabird prediction areas.**

## 6. METHODS

Our goal is to identify alternatives that represent compelling compromises between seabird vulnerability and wind facility performance. Sites that are favorable for having low seabird vulnerability may not perform as well for power generation and vice versa. This section presents methods used for the multi-objective optimization model to investigate the tradeoff between seabird vulnerability and wind facility performance. The specific method used is called Pareto Optimality analysis. This approach is well-suited to examining the tradeoffs between two competing objectives, and it is a common engineering approach to multi-objective decision making. Here the two competing objectives are:

1) Minimize the seabird abundance over 10m (i.e., seabird vulnerability); and

2) Maximize average annual energy production.

Although 3D seabird density estimates were generated for each of the 44 species, the optimization analysis presented in this report focuses on results on aggregates:

- All Modeled Bird Species.
- California Species of Special Concern (CSSC).
- Murrelets listed as Threatened and/or Endangered by the State and/or Federal Government.

In addition to exploring these groupings, a set of optimization analyses considered a single species: Black-footed Albatross. This species was selected for a several reasons. It is abundant enough and within the same FG as the highly endangered Short-tailed Albatross (whose rarity precluded an adequate sample size), it has been proposed for protection under the federal ESA, yet to be finalized (Fish and Wildlife, 2011), and is a California Species of Special Concern. Species in its FG fly by dynamic-soaring, a behavior that increases their potential to fly within RSZs, especially as wind speeds increase. There are other species that occur in the study area, including special status ones such as Hawaiian Petrel, but for which sample sizes are also meager. However, these species won't be specifically treated in this report.

For the sake of simplifying interpretation of figures, the objective of maximizing annual energy production is treated as a minimization of the inverse of annual generation. As a result of this approach alternatives that perform the best are represented as points nearest the plot origin.

Tradeoffs between seabird abundance and power generation were investigated in two distinct analyses. The first analysis examines each of the 5' x 5' grid cells within the study area, for which bird density estimates were made as a possible alternative in the Pareto analysis. Annual generation estimates were developed for a single turbine centered in each of the approximately 1000 cells that are within water depths feasible for mooring floating wind turbines. This analysis serves to look at the tradeoff between power generation and average seabird densities for the entire study area.

In the second analysis, the alternatives considered include each of the selected wind facility locations and build-outs listed in Table 1. For both analyses, energy production is quantified as both the annual total production by the <u>wind facility</u> and the annual total production <u>per turbine</u>. Additionally, the seabird vulnerability metric will be seabird density at risk height (birds/$km^2$). In the case where alternatives have multiple turbines (i.e., wind farms) a total vulnerability metric is also used. This is a simple sum of the estimated seabird density above 10 m at each of the turbine locations, resulting in units of bird-turbines/km$^2$.

The alternatives that fall on the Pareto frontiers can be identified via multiple methods. The method applied here starts by sorting all of the alternatives (i.e. the roughly 1000 5' x 5' mile grid cells for the single-turbine analysis or wind facility locations and build-outs for the wind facility scenarios analysis) by the magnitude of one of the objectives (e.g., sorting annual wind facility energy production from greatest to least) and then examining the points in sequence beginning from an end point:

Let $X_i$ and $Y_i$ represent the paired values of production and vulnerability for each of the n alternatives numbered i = 1 to n, where the $X_i$ values have been sorted so that $X_1$ = maximum ≥ $X_2$ ≥ ...$X_i$ ≥ ... $X_n$ = minimum.

($X_1$, $Y_1$) is an end point for the Pareto frontier (i.e., the upper right X) and the remaining points on the frontier can be identified as follows:

For i = 2 to n

If ($Y_i < \min(Y_1:Y_{i-1})$ ) then ($X_i$, $Y_i$) falls on the frontier

Some post processing of these Pareto optimality results is also done to better understand what tradeoff is made at each cell that falls on or near the Pareto frontier (nearest 20% of solutions). This analysis uses K-means clustering to group alternatives based on their standardized performance in each of the metrics. The centers for these clusters are started on the Pareto front evenly spaced in terms of seabird pseudo weights (Clusters starting at: 0.1, 0.3, 0.5, 0.7 and 0.9). The goal of starting these clusters at different pseudo weight values is to create groupings that show different relative tradeoffs between the two metrics. For example, a cluster started at 0.1 would represent the solutions that favors energy production over seabird vulnerability, while a cluster that started at 0.5 would represent a more balanced tradeoff.

Pseudo-weights are calculated using the relative distance of each alternative to the worst value in each metric (i.e., the maximums for the inverse generation and the bird abundance metrics) to calculate weighting factors. These pseudo-weights always sum to unity for a given cell and are calculated using equation 1 (Carrillo, 2012).

$$W_i = \frac{\frac{\mathrm{BA}_{max} - BA_i}{BA_{max} - BA_{min}}}{\frac{IG_{max} - IG_i}{IG_{max} - IG_{min}} + \frac{\mathrm{BA}_{max} - BA_i}{BA_{max} - BA_{min}}}$$

where:

BA is the bird abundance metric used (total or per turbine, depending on application) (Bird-Turbines/Km$^2$ or Birds / km$^2$, respectively)

IG is the inverse generation (total or per turbine, depending on application) (GWh/year, in both cases)

## 7. Results

The results are presented in three parts,

1. Seabird Density Analyses
   Results of the seabird density precursor analysis, aggregated into the groups used for Pareto optimization.

2. Single Turbine Analyses
   Pareto analysis of the study area considering single turbines located in the center of each cell.

3. Facility Scenario Analyses
   Pareto analysis considering wind facility scenarios shown in Table 1.

### 7.1. Seabird Density Results

This section presents the results of the2D and 3D seabird density analysis for each of the seabird groupings to be explored using the Pareto optimality approach. While following sections will compare seabird density and power generation, this section presents only seabird density. Figures 2 – 5 show theses seabird density results for each of the groupings (or single species) used respectively:

- All Modeled Seabird Species.
- California Species of Special Concern (CSSC).
- Murrelets Listed as Threatened and/or Endangered by the State and/or Federal Government, and
- Black-footed Albatross.

It is important to note that each figure uses a different scaling to represent seabird densities. In all cases red represents the highest densities observed and purple and white shows some of the lowest densities. For example, in Figure 2 (All modeled seabird species) red colored cells represent densities up to ~125 birds/km$^2$ while a red colored cell in Figure 4 (representing State or Federally listed Murrelets) only represents a density of ~1 bird/km$^2$.

With the considered turbine designs, birds would not face risk of collision with turbine blades until they are above about 30m altitude. However, we consider birds predicted to fly above 10 m altitude as being vulnerable in the context of this analysis, due to data limitations. This framing means that our analysis is likely to overestimate the density of birds. Nonetheless, a common feature of all 4 of these figures is that the density of birds above 10 m is only a small portion of the total predicted density. This indicates that even when considering a more conservative risk height of 10 m, most birds flying in a wind facility are not expected to be vulnerable to collision with turbine blades.

The study-area-average ratio of birds above 10m to birds at all altitudes for each of the presented seabird groupings is presented to highlight this point. For the “all modeled seabird species” grouping only 8% of the estimated density occurs above 10m. For CSSC grouped species this only 0.2% of the estimated density is predicted above 10m. For State and Federal listed Murrelets only 0.1% of the estimated density is predicted above 10. Finally, for Black-footed Albatross 5.7% of estimated density is predicted above 10m.

For the groupings that represent species having additional regulatory protections (other than the migratory Bird Protection Act), the maps that show densities above 10m appear empty (right side of Figures 3 and 4). This is because few of the predicted densities exceed the lower limit of the purple cell coloring. The maximum and average of these small values are presented in the top right of these Figures but some cells are visually represented as zeros due to having very low predicted values.

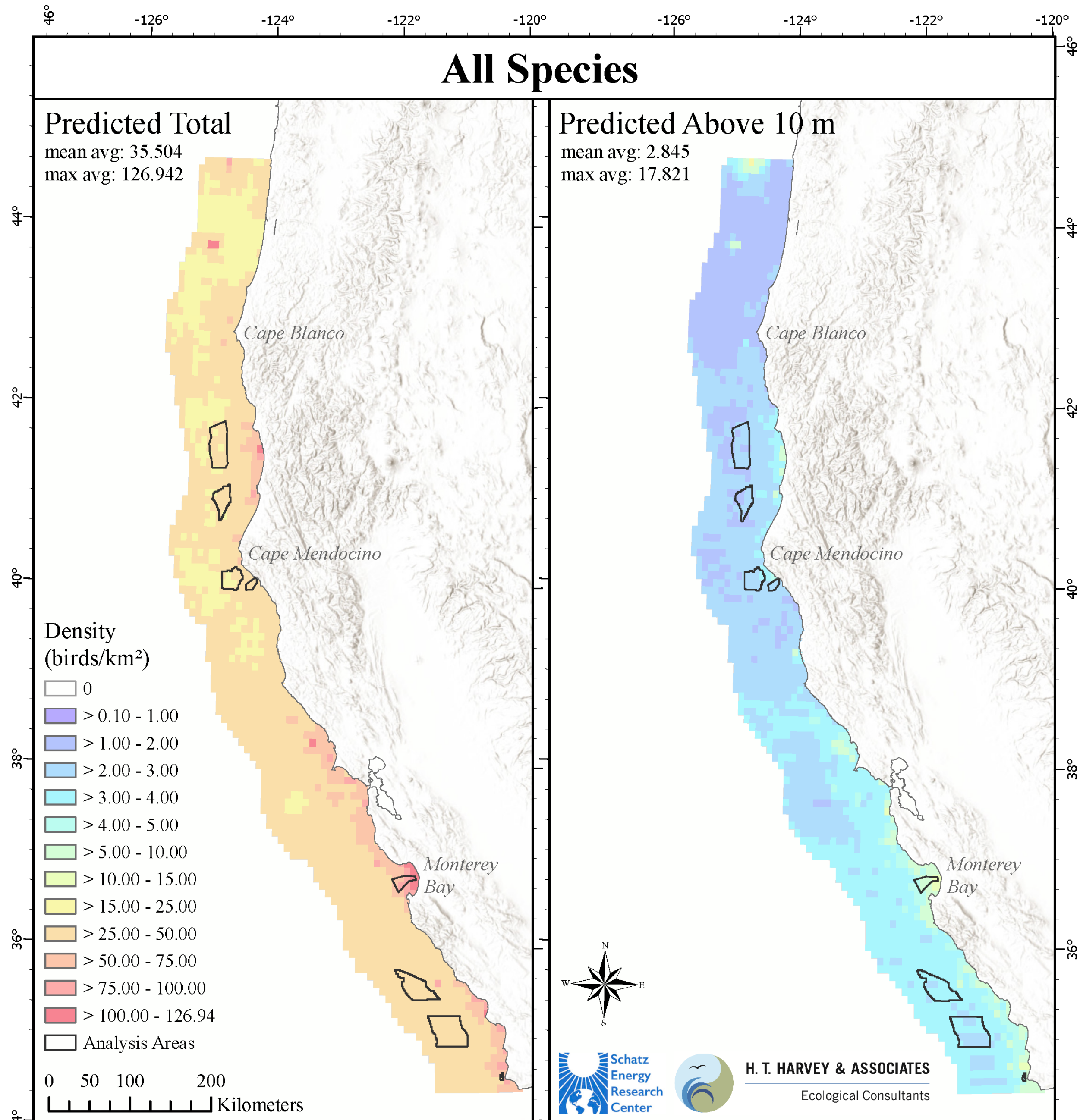


**Figure 2: Spatial predictions of seabird density for all modeled species in the study area. The left panel shows the total estimated seabird density at all altitudes (birds/km²), while the right panel shows seabird density above 10 m, representing birds considered vulnerable to RSZ collisions. Black outlines indicate the Reference Areas investigated in the analysis. The color scale reflects seabird density, with red indicating higher densities and blue/purple indicating lower densities.**

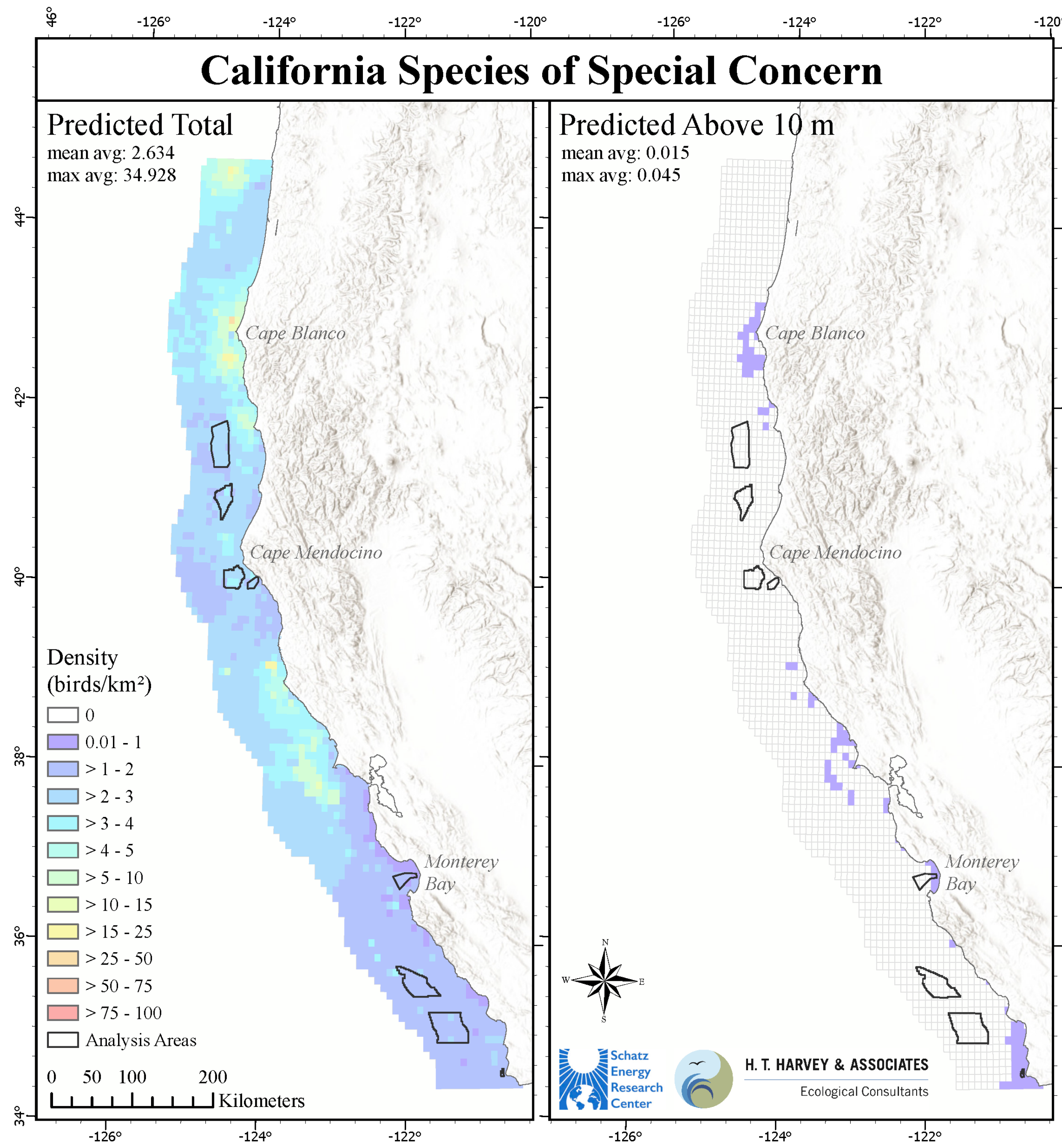


**Figure 3: Spatial predictions of seabird density for California Species of Special Concern (CSSC), including Ashy Storm-Petrel, Fork-tailed Storm-Petrel, Tufted Puffin, Cassin's Auklet, and Common Loon. The left panel shows the total estimated seabird density at all altitudes (birds/km²), while the right panel shows seabird density above 10 m, representing birds considered vulnerable to RSZ collisions. Black outlines indicate the Reference Areas investigated in the analysis. The color scale reflects seabird density, with red indicating higher densities and purple/white indicating lower densities.**

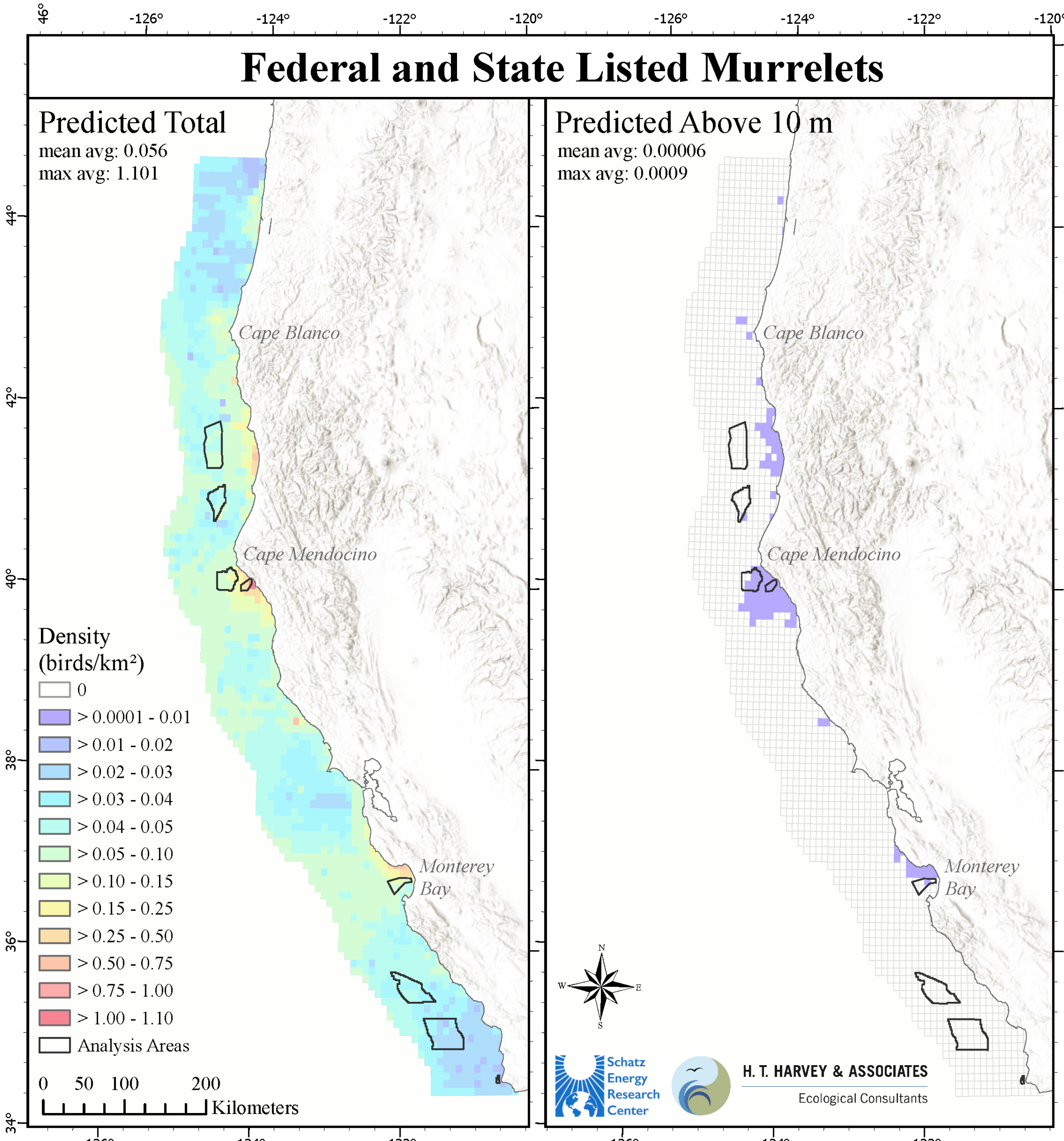


**Figure 4: Spatial predictions of seabird density for murrelets listed as Threatened and/or Endangered by Federal and/or State authorities (Marbled Murrelets and the Scripps's-Guadalupe-Xantus's Murrelet species complex). The left panel shows the total estimated seabird density at all altitudes (birds/km²), while the right panel shows seabird density above 10 m, representing birds considered vulnerable to RSZ collisions. Black outlines indicate the Reference Areas investigated in the analysis. The color scale reflects seabird density, with red indicating higher densities and purple/white indicating lower densities**

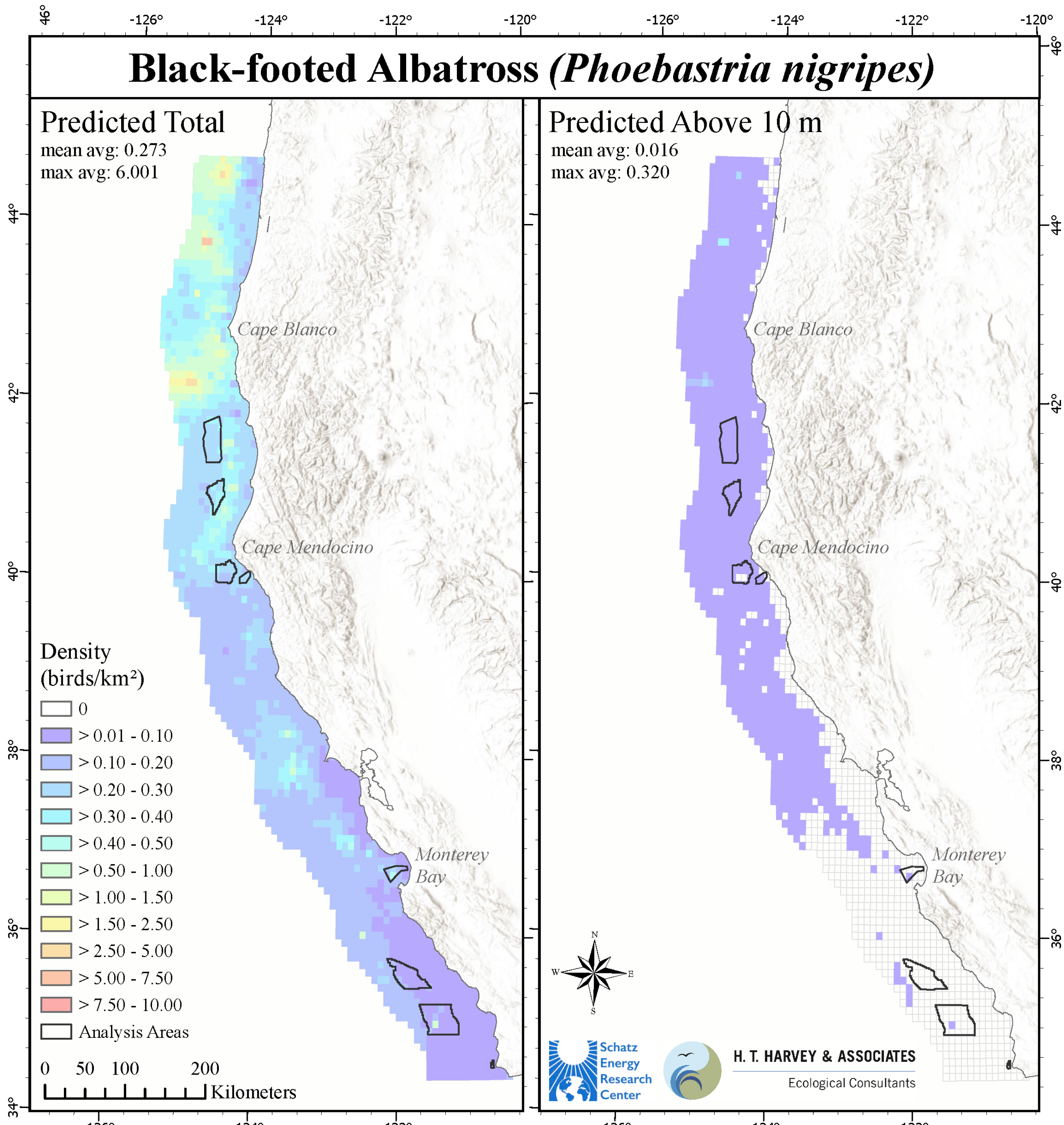


**Figure 4: Spatial predictions of seabird density for Black-footed Albatross (*Phoebastria nigripes*). The left panel shows the total estimated seabird density at all altitudes (birds/km²), while the right panel shows seabird density above 10 m, representing birds considered vulnerable to RSZ collisions. Black outlines indicate the Reference Areas investigated in the analysis. The color scale reflects seabird density, with red indicating higher densities and purple/white indicating lower densities.**

### 7.2. Single Turbine Analysis

This section presents results of the Pareto optimality approach considering alternatives of a single turbine within each cell within the study area. The optimization compares seabird density estimates above 10m altitude with annual energy generation estimates representing a single turbine. Figure 6, below, presents the spatial distribution of the power generation estimates for a single turbine in each cell. These are one of the two variables used in the subsequent optimization plots. Depending on location within the study area, a single turbine would be expected to produce between 8 to 61 Giga-Watt-hours per year, with generation generally increasing with distance from the shore and being the highest in the area west of Cape Mendocino.

Figures 7, 8, 9, and 10 show the Pareto results for all species, California Species of Special Concern, State and Federally listed Murrelets, and the Black-footed albatross, respectively. These figures show the Pareto frontiers established by comparing the inverse of the annual energy production for single turbine scenarios with the estimated bird density above 10m. This is shown in solution space in the top right of the map graphic with points colored to show how far from the Pareto frontier each alternative is. The accompanying (top left) map graphic shows these same alternatives with the same colors but placed spatially. The lower half of these graphics shows a K-means grouping analysis for 20% of the cells that are nearest to the frontier. However, the organization of the two lower panes mirror that of the upper panes. The right graphic shows these alternatives in solution space while the left shows these alternative plotted in a map graphic. As each of these K-means groups were started at different pseudo-weights along the frontier they can be thought of as groups of solutions that might be selected given different weighting of the two objectives and have been labeled to represent this.

In each of the Figures 7 - 10, there is a "knee" in the Pareto curve pointed toward the lower left. The steep slope to the left of the knee and the shallow slope to the right of the knee, make alternatives near the knee look attractive as these alternatives preform relativity well in both metrics. When comparing alternatives that are near the knee to those grouped as “Strong Preference to Power Generation”, there is an increase in bird density (for all species groups) but a relatively modest increase in power generation. A similar statement can be made when comparing alternatives near the knee to those grouped as “Strong Preference to Low Bird Vulnerability, where there is a relatively modest increase in bird density but a significant decrease in power generation

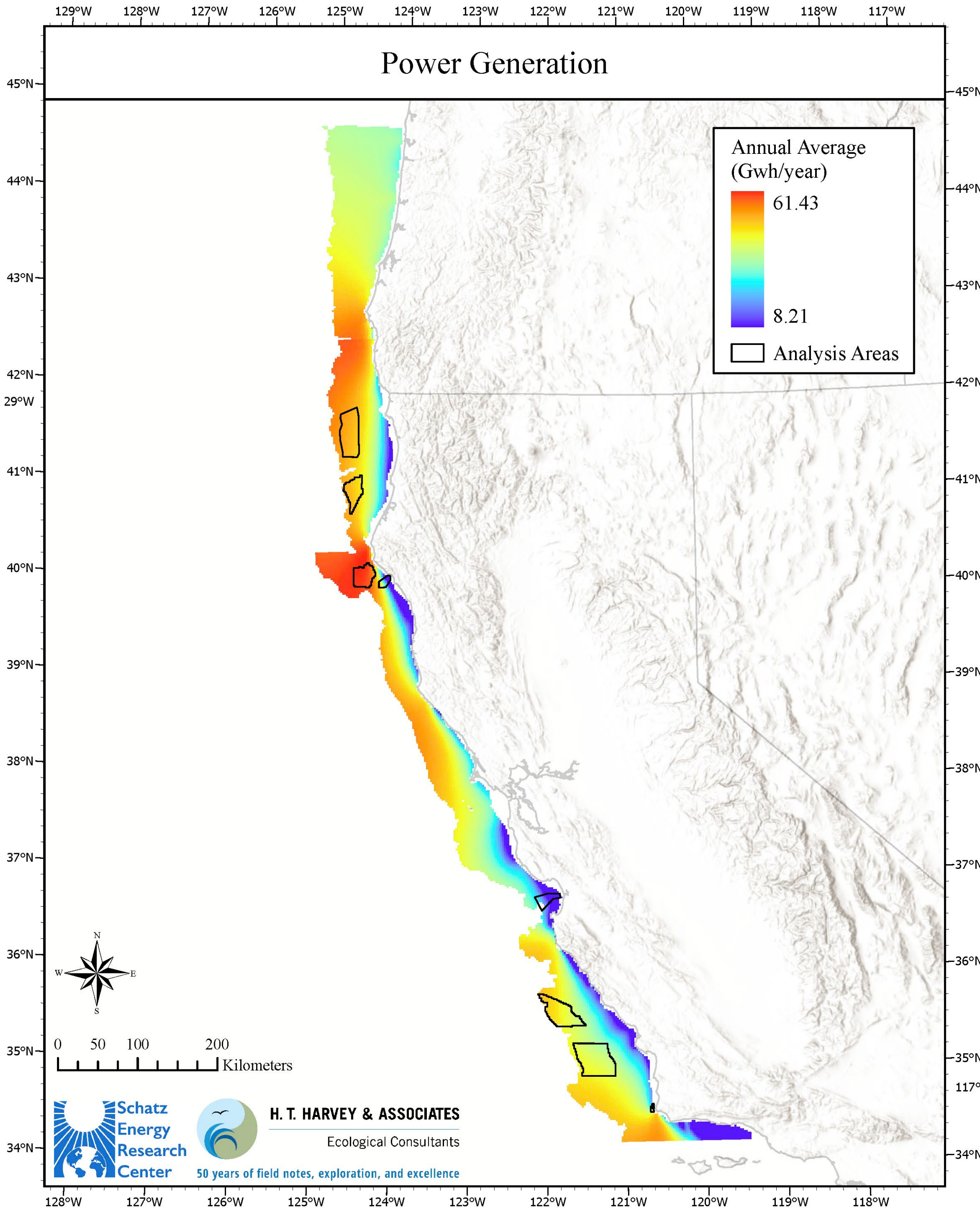


**Figure 5: Average annual generation from a single 12 MW turbine at each of the 1 x 1 km$^2$ within the study area. Warmer colors (e.g., red) represent areas with higher predicted energy generation, while cooler colors (e.g., blue) indicate areas with lower predicted generation. The black outlines represent the borders of the Reference Areas investigated in this study. These estimates provide a spatial understanding of the wind energy potential across the California coast**

*All Seabirds included in the Framework*

The "All Species" Pareto analysis (Figure 7) illustrates the trade-offs between seabird density at RSZ height (above 10 m) and annual energy generation across the study area. The results indicate that higher seabird densities generally correspond to lower power generation, with bird densities above 10 m ranging from 1 to over 15 birds/km$^2$. The maximum predicted annual energy generation per turbine is around 20 GWh, typically in areas with lower bird densities (under 5 birds/km$^2$) (Figure 7, upper panel). Spatial patterns reveal that nearshore regions, particularly around Monterey Bay, have higher concentrations of birds flying above 10 m and lower power generation potential, making them less suitable for wind development. Offshore areas near Cape Mendocino, however, offer higher power generation potential and lower seabird densities, positioning these locations closer to the Pareto frontier. The cluster analysis of the nearest 20% of cells (Figure 7, bottom panel) highlights the areas that would be selected given different objective weights between seabird conservation and energy generation, with areas near Cape Mendocino favoring energy production and areas to the north of the study area favoring low bird vulnerability. The “knee” in the Pareto curve, shown near the yellow grouping, marks an attractive balance between these two objectives. The 20% of cells nearest the Pareto frontier were all located from Cape Mendocino northward (Figure 7, bottom panel).

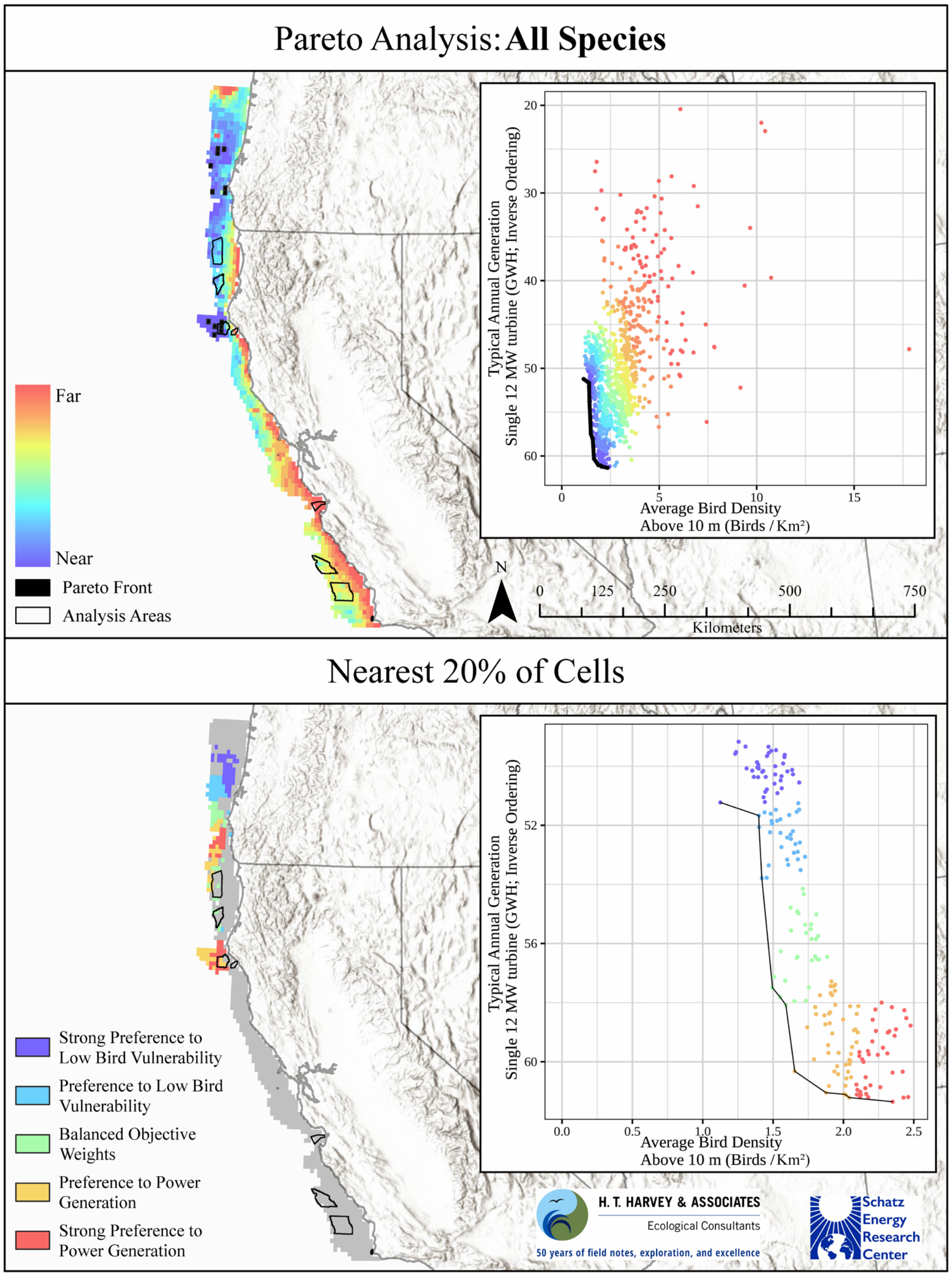


**Figure 6: Pareto analysis results for all modeled seabird species, showing trade-offs between bird vulnerability and wind energy production. The left map shows how each grid cell is positioned in relation to the Pareto front, with "near" cells (blue to purple) being closest to the optimal balance of low bird vulnerability and high power generation. The inset graph compares the typical annual energy generation (GWh/year) from a single 12 MW turbine to the average seabird density above 10 meters. The right map (bottom) focuses on the nearest 20% of cells to the Pareto front, highlighting preference clusters ranging from strong preference for low bird vulnerability (purple) to strong preference for power generation (red).**

*California Species of Special Concern*

The CSSC Pareto analysis (Figure 8) presents similar trade-offs between bird density at RSZ height (above 10 m) and annual energy generation, but with distinct patterns compared to the "All Species" analysis. In the CSSC analysis, bird densities above 10 m are much lower, ranging from nearly 0 to just over 0.04 birds/km², compared to the much higher densities in the "All Species" results (up to 15 birds/km²). This suggests that CSSC species are less prevalent at RSZ heights.

Spatially, the regions around Humboldt County, north of Cape Mendocino, exhibit the best balance of low seabird vulnerability and high energy generation potential, highlighting this area as attractive for wind development. The "knee" in the Pareto curve for CSSC species is located at much lower bird densities than the "All Species" curve, around 0.001–0.003 birds/km². This indicates that, for CSSC species, even the areas with higher energy potential have relatively low bird density.

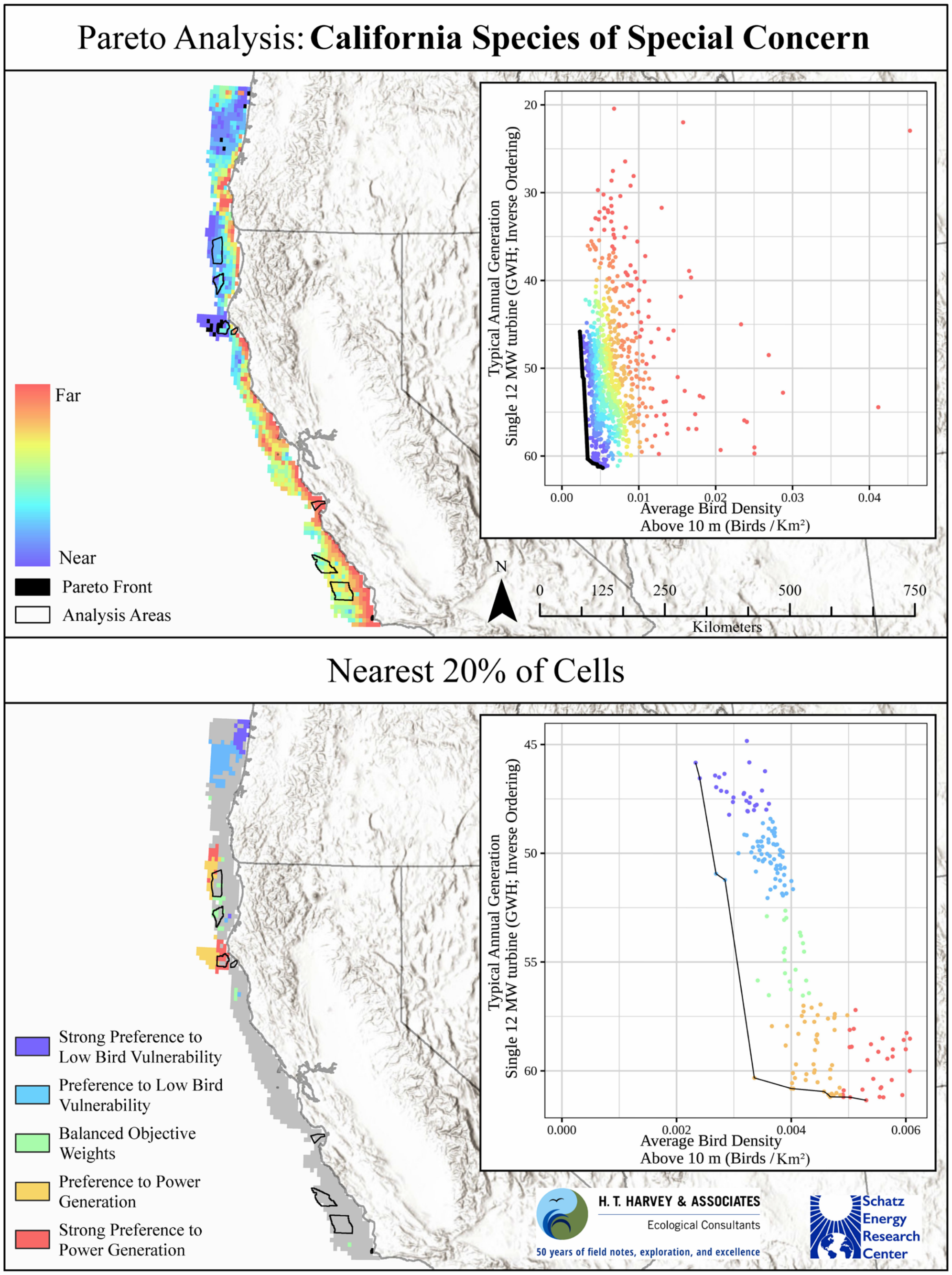


**Figure 7: Pareto analysis results for all modeled seabird species, showing trade-offs between bird vulnerability and wind energy production. The left map shows how each grid cell is positioned in relation to the Pareto front, with "near" cells (blue to purple) being closest to the optimal balance of low bird vulnerability and high power generation. The inset graph compares the typical annual energy generation (GWh/year) from a single 12 MW turbine to the average seabird density above 10 meters. The right map (bottom) focuses on the nearest 20% of cells to the Pareto front, highlighting preference clusters ranging from strong preference for low bird vulnerability (purple) to strong preference for power generation (red).**

*ESA-Listed Murrelets*

The Pareto analysis for ESA-listed murrelets (Figure 9) reveals extremely low seabird densities at RSZ height (above 10 m), with values ranging from nearly zero to approximately 0.0001 birds/km². This indicates that over 99.9% of the murrelet population remains below RSZ heights, greatly reducing the risk of turbine collisions for this species.

The analysis shows that the highest energy production areas, yielding up to around 20 GWh per turbine, are associated with minimal murrelet densities. Spatially, the best areas for wind energy development, identified as having "Balanced Objective Weights," are located off Central and Southern California. The green patches in these regions indicate optimal trade-offs between wind energy generation and low murrelet vulnerability. Although due to murrelets Flight style and minimal presense further from shore most sites seriouly considered for OSW have low densitys of these birds.

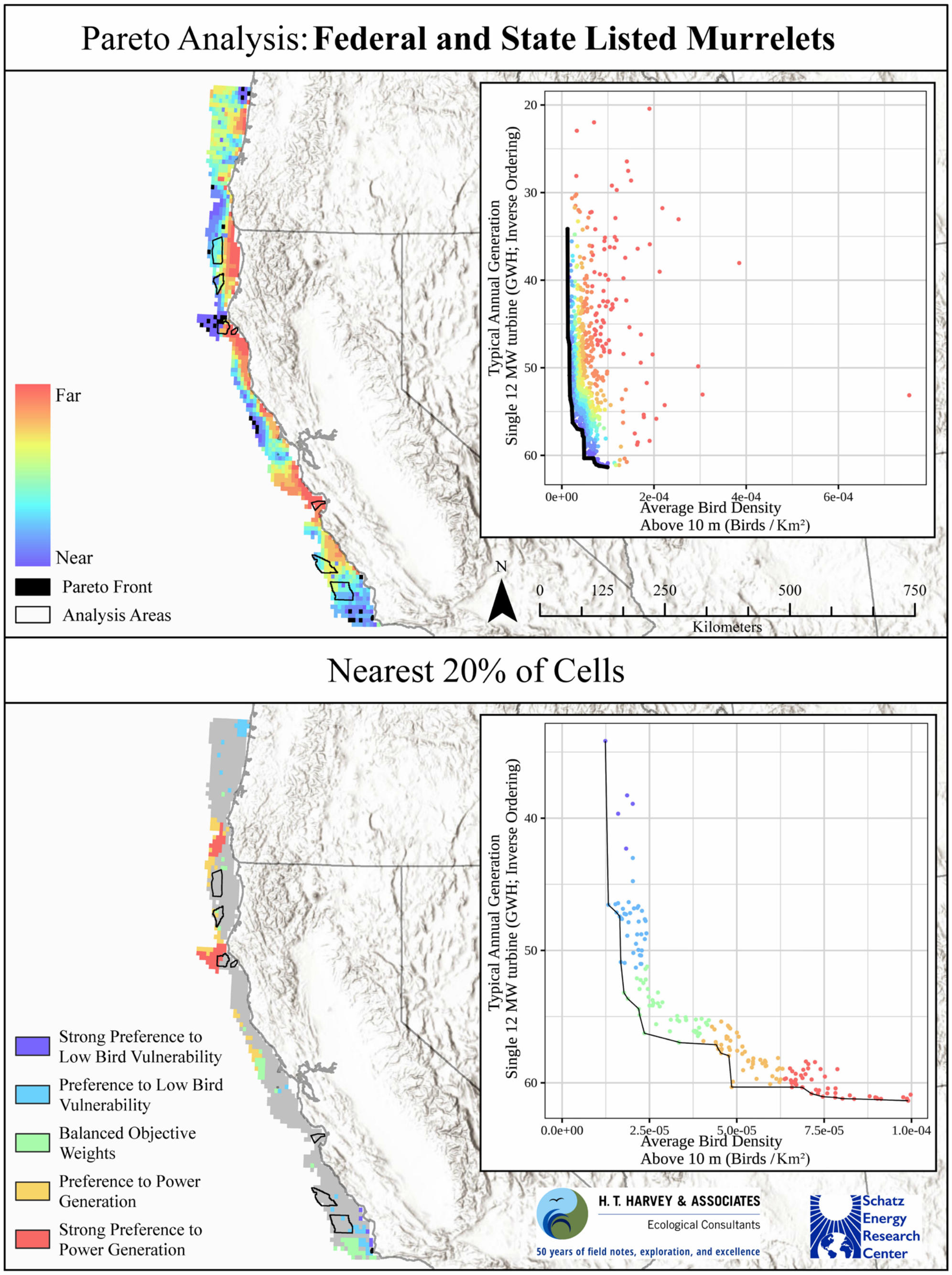


**Figure 8: Pareto analysis results for murrelet species included on Federal and/or State Threatened and/or Endangered Species Lists (ESA-listed), showing trade-offs between bird vulnerability and wind energy production. The left map shows how each grid cell is positioned in relation to the Pareto front, with cells nearer the optimal balance of low bird vulnerability and high power generation shown in blue to purple. The inset graph compares typical annual energy generation (GWh/year) from a single 12 MW turbine to the average density of murrelets flying above 10 meters. The right map (bottom) focuses on the nearest 20% of cells to the Pareto front, highlighting preference clusters ranging from strong preference for low bird vulnerability (purple) to strong preference for power generation (red).**

*Black-footed Albatross*

The Pareto analysis for the Black-footed Albatross (Figure 10) displays notably different patterns compared to the other species analyzed. Black-footed Albatross densities above 10 m are slightly higher than those for California Species of Special Concern (CSSC) species, with values ranging from near zero to approximately 0.03 birds/km$^2$. While this density is still low, it is much greater than those of ESA-listed murrelets, suggesting that Black-footed Albatross are more likely to fly at RSZ heights and may have greater collision risk with turbines.

The most striking feature of the Pareto analysis for the Black-footed Albatross is the very steep slope of the Pareto curve, with a clear lack of cells clustering at the bend in the curve. Unlike the broader seabird community or CSSC species, where multiple cells are positioned along the Pareto front (near the balance between bird vulnerability and energy generation), the Black-footed Albatross analysis shows only a single cell in the bottom panel close to the “knee” of the Pareto curve. This indicates that for Black-footed Albatross, very few sites have desirable performance in both metrics.

Spatially, the best areas that balance bird vulnerability and power generation (indicated by the green cells in the bottom panel) are mostly offshore, concentrated in the south of the study area. These regions offer a favorable trade-off for Black-footed Albatross conservation and wind energy development.

Overall, the distinct shape of the Pareto curve in the Black-footed Albatross analysis highlights how much more difficult it is to find areas that optimize both objectives compared to other species groups. The steeper curve and the fact that only a single cell lies near the “knee” further emphasize that the trade-offs are sharper, with fewer opportunities to meet both goals simultaneously.

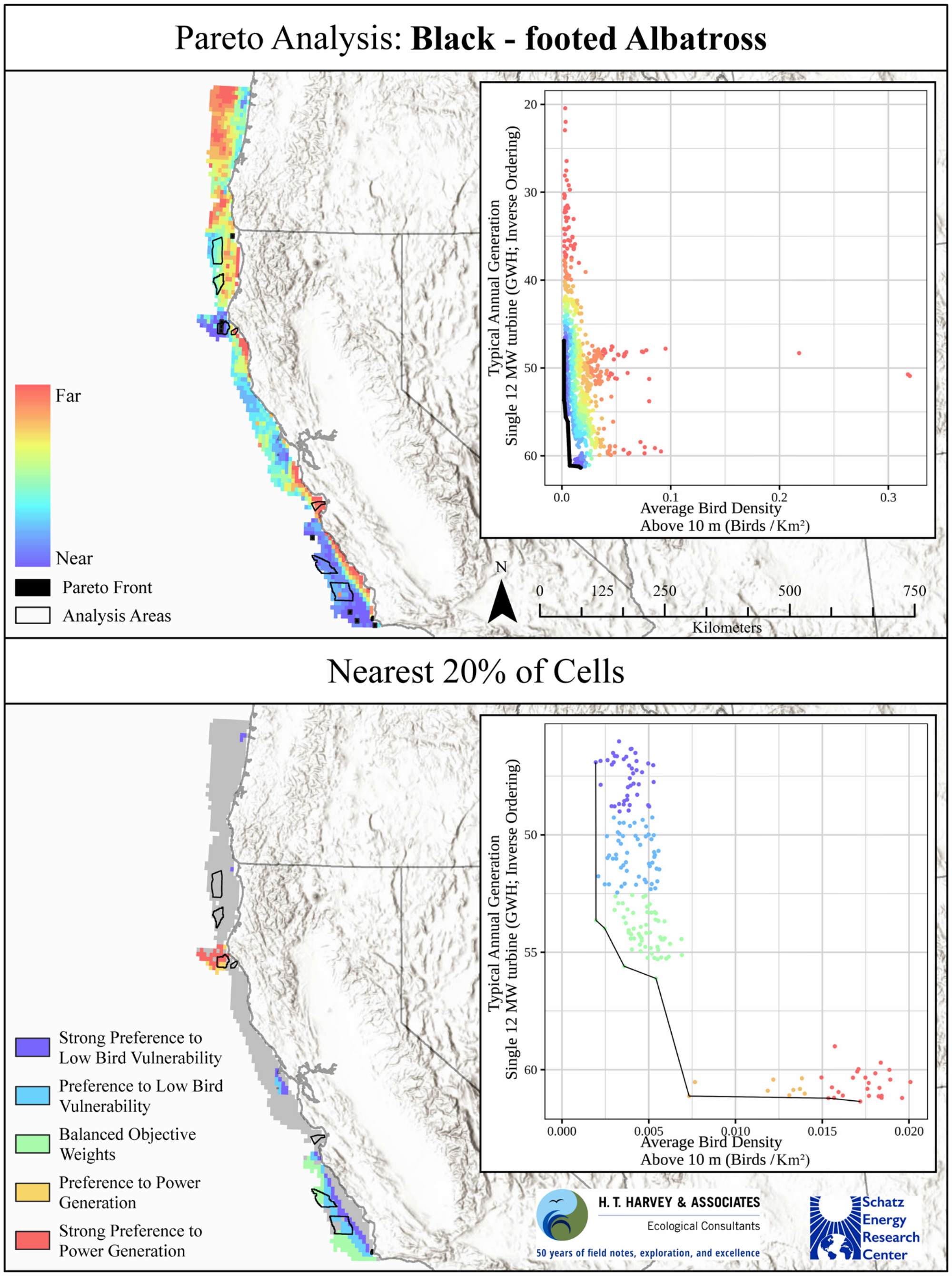


**Figure 9: Pareto analysis results for the Black-footed Albatross, illustrating trade-offs between bird vulnerability and wind energy production. The left map shows how each grid cell is positioned relative to the Pareto front, with "near" cells (blue to purple) being closest to the optimal balance of low bird vulnerability and high power generation. The inset graph compares the typical annual energy generation (GWh/year) from a single 12 MW turbine to the average density of Black-footed Albatross above 10 meters. The right map (bottom) focuses on the nearest 20% of cells to the Pareto front, highlighting preference clusters ranging from strong preference for low bird vulnerability (purple) to strong preference for power generation (red).**

### 7.3. Facility Scenario Analysis

The following section serves to compare the estimated annual energy production of 32 wind facility scenarios with seabird vulnerability metrics. Two sets of figures are presented; the first trades-off total vulnerability and energy generation while the second uses per turbine metrics. Per turbine metrics are better for directly comparing the estimated seabird density in two locations but do not account for the difference in possible buildout sizing between locations. Without accounting for possible avoidance behaviors, for a given area the larger the number of turbines, the greater the hazard to birds. The total vulnerability metric takes into account these different buildouts levels for different areas but this leads to the simple conclusion that smaller facilities pose less threat to seabirds.

While scenarios for both 12 and 15 MW turbines were explored, direct comparisons between these different nameplate capacities are unfortunately not possible, because the seabird vulnerability metric used here is defined as the density of seabirds >10m at the turbine location. Consequently, this metric cannot account for the increased risk assumed to be associated with the larger rotor diameter of the 15 MW turbine. Instead, this report focuses on results from 12 MW scenarios only.

The core figures in this section use 1-2 letter abbreviations to relate points (in solution space) to the geographic areas studied. Figure 1, above, shows where the planned and hypothetical wind facility analysis areas are located, the abbreviations used for each area, the 1300m and 3000m depth contours, and the seabird prediction area.

#### *7.3.1. Full Facility (Additive) Performance Metrics*

Figures 11 - 14 depict tradeoffs between total vulnerability and total energy generation for wind facility full build-out scenarios. Annual energy generation for the entire wind facility is calculated and seabird density estimates at each turbine location are summed to provide total bird vulnerability in units of birds-turbines / km$^2$. Within this analysis, because the sum of each metric is used, larger facilities perform better in the power generation metric and worse in the seabird vulnerability metric. As such we exclude the very small facilities (CADEMO and Vandenburg) from this analysis as the low turbine counts position these facilities as outliers providing far less total generation and far less estimated total vulnerability.

This analysis is completed for each of the four bird groupings. Because the wind facility sizes examined are the same for all species groups, the vertical scale and the vertical positions of the wind facility alternatives are the same in all four figures. The X-axis scales vary dramatically among the four bird groupings, with a maximum of 1500 birds-turbines / km$^2$ for all species, about 7 birds-turbines / km$^2$ for the Black-footed albatross, 3 birds-turbines / km$^2$ for California Species of Special Concern, and about 0.03 birds-turbines / km$^2$ for Federally or State listed Murrelets. In addition, the Pareto frontiers shown in Figure 11 for all species and Figure 12 for California Species of Special Concern show a similar, almost-linear trade-off pattern among the wind facility sites, with Humboldt in the upper left (lower generation but lower vulnerability) and Diablo Canyon in the lower right (greater generation but higher vulnerability). By contrast, the frontier shown in Figure 13 for Federally or State listed species is almost vertical with little variation in vulnerability across the range of power generation. The frontier shown for the Black-footed Albatross includes only two wind facility alternatives. Tables 3 and 4 present these results.

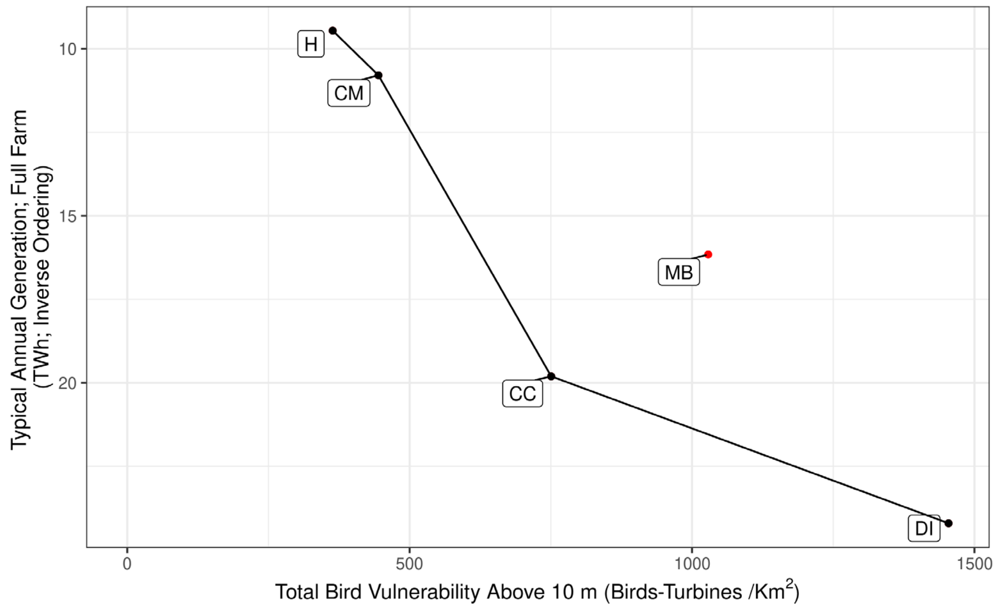


**Figure 10: Pareto Curve comparing total vulnerability of all 44 seabird taxa modeled in the 3D Seabird Framework with wind facility generation under full build-out scenarios using 12 MW turbines. Metrics represent cumulative sums of bird vulnerability and power generation across all turbines within each facility.**

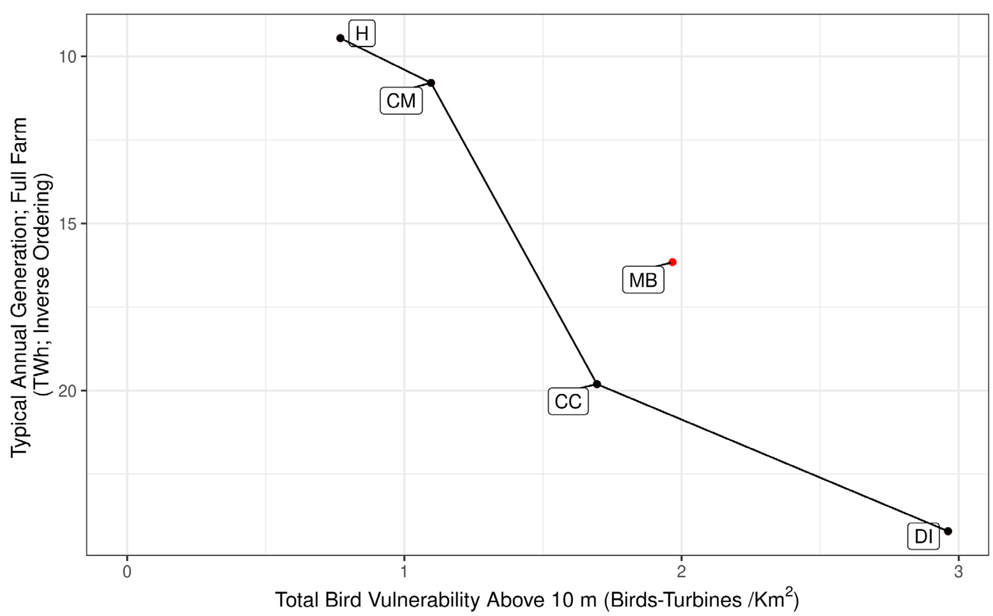


**Figure 11: Pareto Curve comparing total vulnerability of California Species of Special Concern (CSSC) included in the 3D Seabird Framework with wind facility generation under full build-out scenarios using 12 MW turbines. Metrics represent cumulative sums of bird vulnerability and power generation across all turbines within each facility**

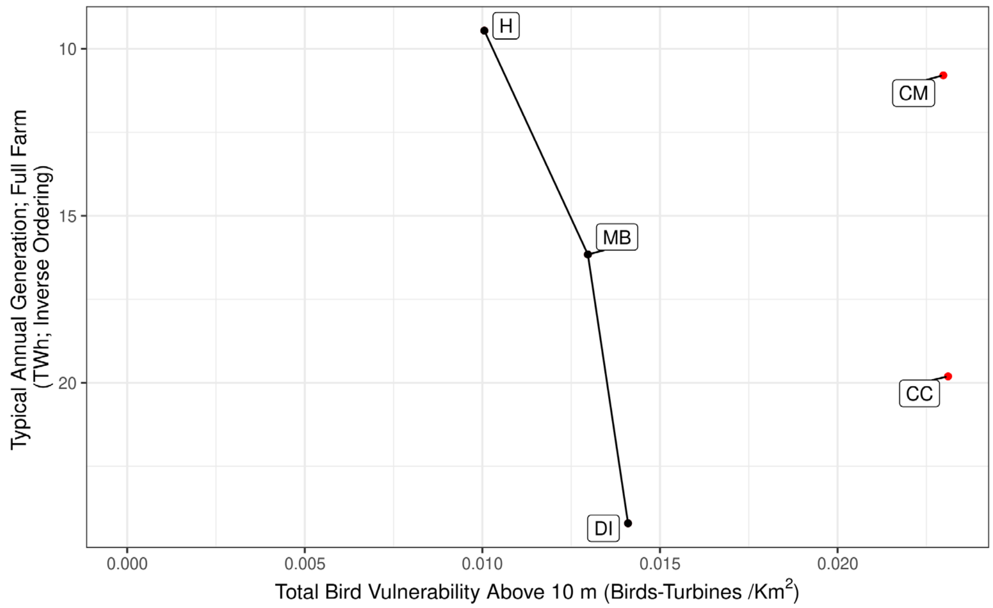


**Figure 12: Pareto Curve comparing total vulnerability of all ESA-listed murrelets included in the 3D Seabird Framework with wind facility generation under full build-out scenarios using 12 MW turbines. Metrics represent cumulative sums of bird vulnerability and power generation across all turbines within each facility.**

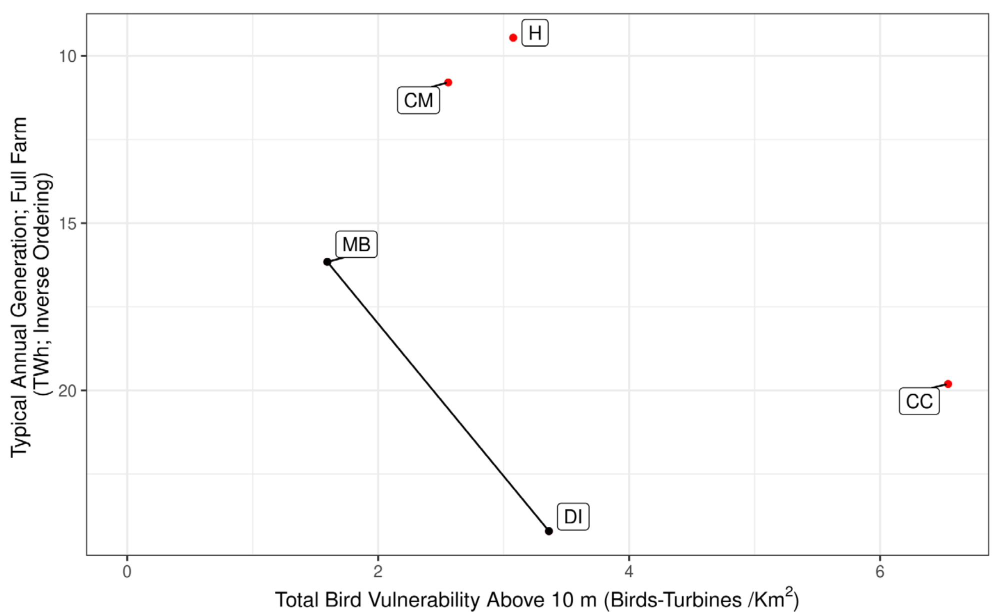


**Figure 13 Pareto Curve comparing total vulnerability of Black-footed Albatross included in the 3D Seabird Framework with wind facility generation under full build-out scenarios using 12 MW turbines. Metrics represent cumulative sums of bird vulnerability and power generation across all turbines within each facility.**

**Table 2: Facility total performance metrics for full buildout facilities (using 12 MW turbines), Bird densities considering only birds above 10m.**

| Location | Nameplate Rating (MW) | Annual Generation (TWh) | Total Vulnerability (bird- turbines/ km²): All Species | Total Vulnerability (bird- turbines/ km²): CSSC | Total Vulnerability (bird- turbines/ km²): ESA listed | Total Vulnerability (bird- turbines/ km²): Black-footed Albatross |
|---|---|---|---|---|---|---|
| **Cape Mendocino** | 2,184 | 10.8 | 440 | 1.1 | 0.023 | 2.6 |
| **Crescent City** | 4,356 | 19.8 | 750 | 1.7 | 0.023 | 6.5 |
| **Diablo Canyon** | 5,928 | 24.2 | 1,500 | 3.0 | 0.014 | 3.4 |
| **Humboldt** | 2,112 | 9.5 | 360 | 0.77 | 0.010 | 3.1 |
| **Morro Bay 376** | 3,816 | 16.2 | 1,000 | 2.0 | 0.013 | 1.6 |

**Table 3: Facility total performance metrics for full buildout facilities (using 12 MW turbines), Bird densities consider birds at all altitudes.**

| Location | Nameplate Rating (MW) | Annual Generation (TWh) | Total Vulnerability (bird- turbines/ km²): All Species | Total Vulnerability (bird- turbines/ km²): CSSC | Total Vulnerability (bird- turbines/ km²): ESA listed | Total Vulnerability (bird- turbines/ km²): Black-footed Albatross |
|---|---|---|---|---|---|---|
| **Cape Mendocino** | 2,184 | 10.8 | 4,900 | 500 | 18 | 38 |
| **Crescent City** | 4,356 | 19.8 | 10,000 | 830 | 18 | 99 |
| **Diablo Canyon** | 5,928 | 24.2 | 17,000 | 740 | 14 | 58 |
| **Humboldt** | 2,112 | 9.5 | 5,000 | 400 | 8.4 | 53 |
| **Morro Bay 376** | 3,816 | 16.2 | 11,000 | 480 | 12 | 26 |

### *7.3.2. Per Turbine Performance Metrics*

Figures 15 - 18 present per turbine average values for both seabird density and power generation for each of the wind facility scenarios. By looking at these on a per turbine basis rather than by total wind facility metrics, this analysis focuses on identifying the location with the best estimated performance for a given wind facility capacity. These figures are generated assuming the same 600MW capacity at each of the locations.

This analysis is completed for each of the four bird groupings. Because the wind facility size for each site examined was 600MW, the annual energy generation only differs among the sites due to the differences in the wind resource. Since that resource is the same for all species groups, the vertical scale and the vertical positions of the wind facility alternatives are equivalent. However, the X-axes scales vary dramatically among the four bird groupings, with a maximum of 7 birds/km$^2$ for all species, 0.018 birds/km$^2$ for the Black-footed Albatross, 0.016 birds/km$^2$ for California Species of Special Concern, and 0.00035 birds/km$^2$ for Federally or State listed Murrelets.

In addition, the Pareto frontier shown in Figure 15 for all species only contains two sites: Crescent City (CC) and Cape Mendocino (CM) with Humboldt (H) nearby. In Figure 16, the frontier for California Species of Special Concern contains H, CC, and CM. The frontier shown in Figure 17 for State and Federally listed species contains seven sites: Vandenberg (V), CADEMO (CA), Diablo Canyon (DI), Moro Bay (MB), Humboldt (H), Crescent City (CC), and Cape Mendocino (CM). Finally, the frontier shown in Figure 18 for the Black-footed albatross contains CA, MB, and CM. See summaries in tables 5 and 6.

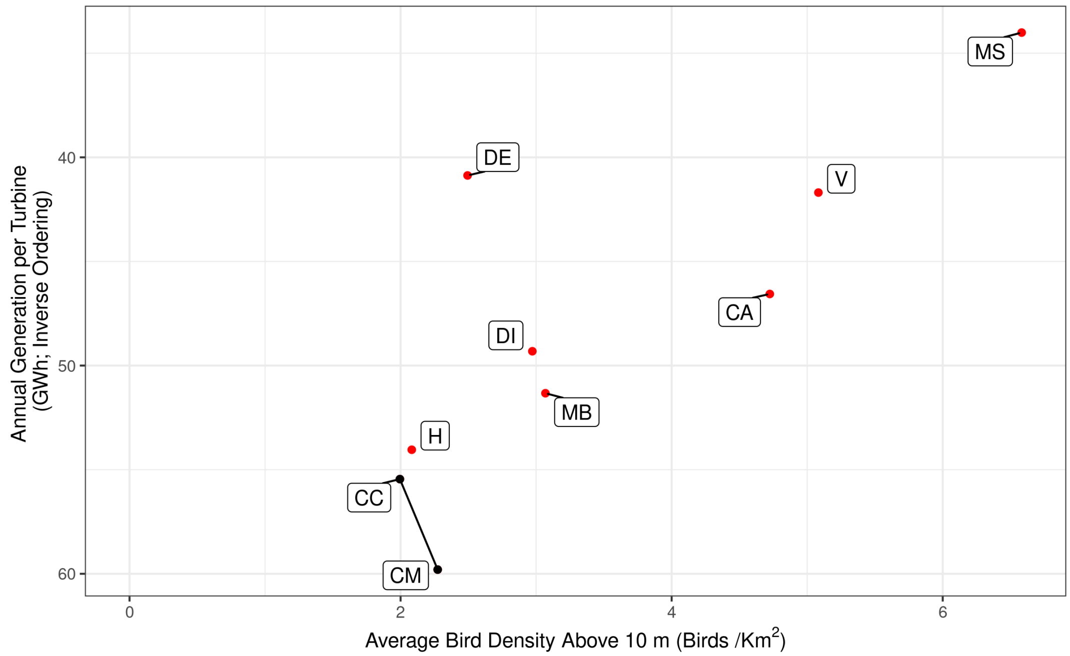


**Figure 14: Pareto Curve comparing average bird density of all modeled bird species with wind facility generation from 600MW scenarios with 12 MW turbines. Metrics represent averages among all turbines.**

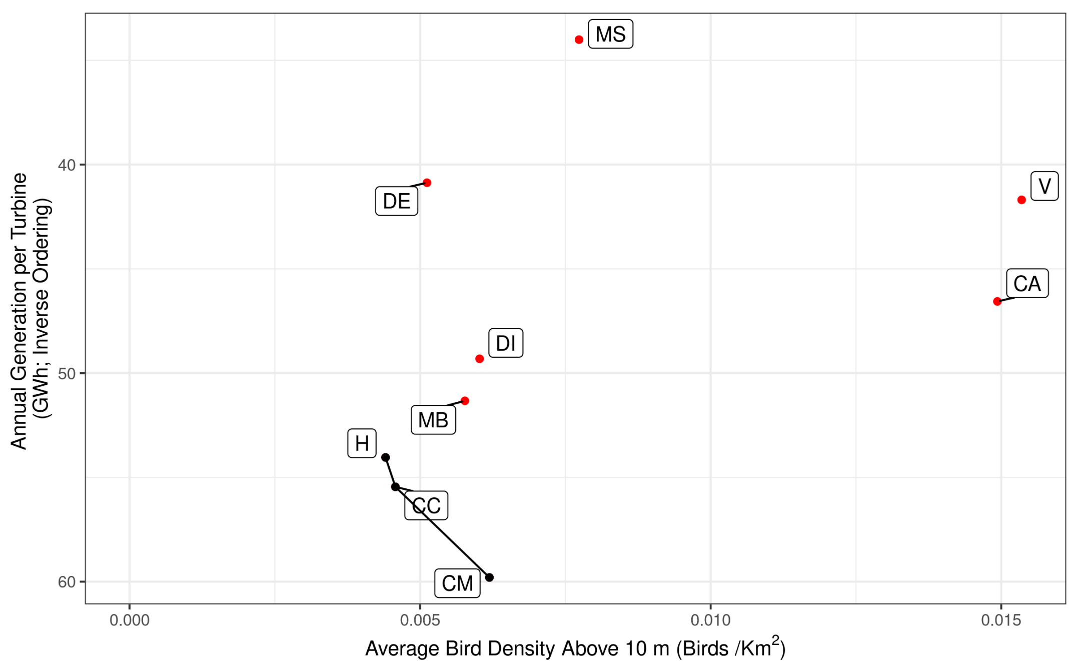


**Figure 15: Pareto Curve comparing average bird density of all modeled bird species listed as a California Species of Special Concern (CSSC) with wind facility generation from 600MW scenarios with 12 MW turbines. Metrics represent averages among all turbines.**

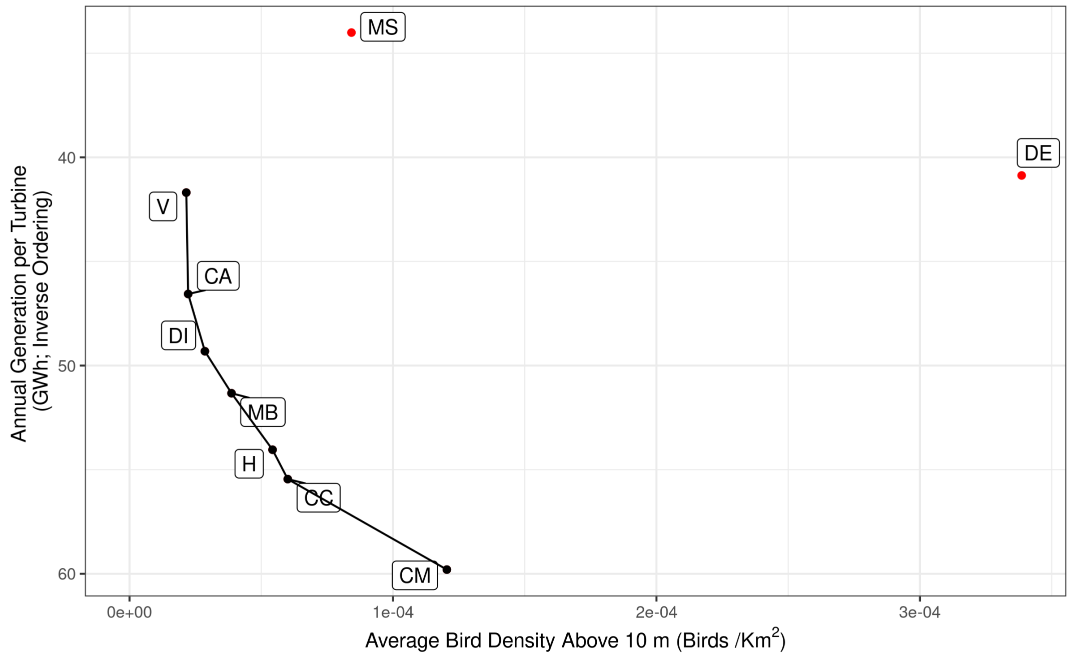


**Figure 16: Pareto Curve comparing average bird density of all modeled bird species that are Federally or State listed with wind facility generation from 600MW scenarios with 12 MW turbines. Metrics represent averages among all turbines**

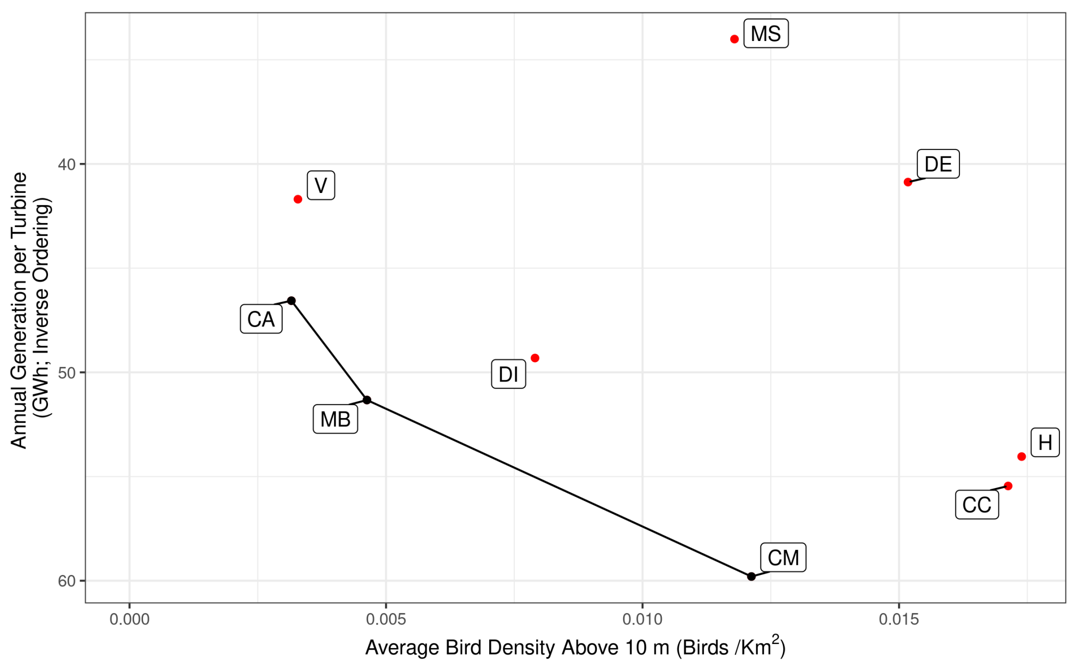


**Figure 17: Pareto Curve comparing average bird density of Black-footed Albatross with wind facility generation from 600MW scenarios with 12 MW turbines. Metrics represent averages among all turbines.**

**Table 4: Per turbine performance metrics for 600 MW farms, Bird densities considering only birds above 10m.**

| Location | Abbreviation | Generation Per Turbine (GWh/Year) | Average Bird Density (Bird/ km$^2$): All Species | Average Bird Density (Bird/ km$^2$): CSSC | Average Bird Density (Bird/ km$^2$): Federal and State Listed | Average Bird Density (Bird/ km$^2$): Black-footed Albatross |
|---|---|---|---|---|---|---|
| **CADEMO** | CA | 46.6 | 4.7 | 1.5E-02 | 2.2E-05 | 3.2E-03 |
| **Cape Mendocino** | CM | 59.8 | 2.3 | 6.2E-03 | 1.2E-04 | 1.2E-02 |
| **Crescent City** | CC | 55.5 | 2.0 | 4.6E-03 | 6.0E-05 | 1.7E-02 |
| **Delgada Canyon** | DE | 40.9 | 2.5 | 5.1E-03 | 3.4E-04 | 1.5E-02 |
| **Diablo Canyon** | DI | 49.3 | 3.0 | 6.0E-03 | 2.9E-05 | 7.9E-03 |
| **Humboldt** | H | 54.0 | 2.0 | 4.4E-03 | 5.4E-05 | 1.7E-02 |
| **Monterey System** | MS | 34.0 | 6.6 | 7.7E-03 | 8.4E-05 | 1.2E-02 |
| **Morro Bay 376** | MB | 51.3 | 3.1 | 5.8E-03 | 3.9E-05 | 4.6E-03 |
| **Vandenburg (AFPP)** | V | 41.7 | 5.1 | 1.5E-02 | 2.2E-05 | 3.3E-03 |

**Table 5: Per turbine performance metrics for 600 MW, Bird densities considering birds at all altitudes.**

| Location | Abbreviation | Generation Per Turbine (GWh/Year) | Average Bird Density (Bird/ km$^2$): All Species | Average Bird Density (Bird/ km$^2$): CSSC | Average Bird Density (Bird/ km$^2$): Federal and State Listed | Average Bird Density (Bird/ km$^2$): Black-footed Albatross |
|---|---|---|---|---|---|---|
| **CADEMO** | CA | 46.6 | 49.6 | 1.3 | 6.4E-02 | 2.3E-02 |
| **Cape Mendocino** | CM | 59.8 | 25.1 | 3.0 | 1.8E-01 | 9.5E-02 |
| **Crescent City** | CC | 55.5 | 27.7 | 2.3 | 2.6E-01 | 4.6E-02 |
| **Delgada Canyon** | DE | 40.9 | 30.1 | 2.0 | 2.4E-01 | 3.2E-01 |
| **Diablo Canyon** | DI | 49.3 | 34.1 | 1.5 | 1.4E-01 | 2.8E-02 |
| **Humboldt** | H | 54.0 | 29.1 | 2.3 | 3.0E-01 | 4.5E-02 |
| **Monterey System** | MS | 34.0 | 76.3 | 1.0 | 2.5E-01 | 1.0E-01 |
| **Morro Bay 376** | MB | 51.3 | 33.1 | 1.4 | 7.7E-02 | 3.7E-02 |
| **Vandenburg (AFPP)** | V | 41.7 | 53.9 | 1.4 | 7.0E-02 | 2.3E-02 |

## 8. Conclusion

The multi-objective optimization presented in this report is the culmination of multiple analytical efforts to quantify the trade-off between seabirds' risk of collision (quantified using density of seabirds above 10m) and potential energy generation from floating offshore wind turbines. This work addresses a key gap in the understanding of this tradeoff that no other work we are aware of addresses: the vertical component to seabirds' flight. Other studies which aim to predict seabird densities only estimate their distribution in two dimensions (Nur et al., 2011; Adams et al., 2017; Leirness et al. 2021).

Seabird activity in the study area is largely below 10m altitude, while turbine blades are expected to reach no lower than about 30m above the water line. Since data limitations prevented quantifying seabird densities above 30m, instead seabirds observed above 10m were considered vulnerable to collision in this framework. This inherent bias to the analysis means that the estimated 8% of the seabird density above 10m is likely an overestimate of seabirds vulnerable to collision, as in reality an even smaller portion of the seabirds would be present above 30m. However other factors may have also biased this work including the limitations of human observers. When considering subsets of the species modeled that have legal protections, this ratio is even lower. For California Species of Special Concern, only 0.2% of seabird density is predicted to be above 10m. For Murrelets listed at the State and/or Federal level, only 0.1% are estimated above 10m. And for the Black-footed Albatross this value is 5.7%.

Also note that seabirds with additional regulatory protections make up only a small portion of the overall seabird community. This can best be observed in Figures 2 – 5. In Figure 2 that presents results for all 44 modeled seabird species, red colored cells represent the highest estimated densities and range up to ~125 birds per square kilometer. In contrast, a red colored cell in Figure 4, which presents results for State or Federally listed Murrelets, only represents a density of ~1 bird per square kilometer, smaller by a factor of over 100.

Looking to the Pareto front graphics, we can see that near-shore areas typically perform poorly, falling far from the Pareto front. These near shore areas are estimated to have higher concentrations of seabirds at risk height than offshore areas (Figures 2 – 5) as well as lower power generation (Figure 6), which shows that these two objectives are not in strong conflict in the area of study.

The Pareto curves for single turbine scenarios (Figures 7-10; top right pane) also demonstrate that these objectives are largely not in conflict. The "elbow" or "knee" (turning point in the Pareto front curve) is near to the origin. The alternatives that fall in the knee of the Pareto curve and are closest to the origin have good performance in both metrics, with annual energy generation that is relatively near to the maximum observed and seabird density above 10m that is relative near to the minimum observed. If these two objectives were largely at conflict, we would see a concave shape to the Pareto curves.

The optimization that looked at per turbine metrics for wind facility scenarios showed that the Crescent City, Cape Mendocino and Humboldt locations performed the best (Figures 15 – 18). These locations fell on or near to the Pareto front for three of the examined seabird groupings, with the exception being the Black-footed Albatross that is more concentrated in the north of the study area.

The optimization that looked at full facility (additive metrics) for wind facility scenarios shows wind facilities with more turbines generate more energy annually but are also would be a larger collision vulnerability. The metrics used for quantifying bird vulnerability in this study are however simple additive metrics which sum the density of seabirds predicted at each turbine location. Ideally, to best compare these different buildout sizes, the vulnerability metric used would account for flight paths and passage rates of seabirds, to more accurately represent the vulnerability associated with different size farms. However, the available data for seabirds on the U.S. West Coast has yet to become sophisticated enough to enable such an analysis. One driving factor of this lack of data is that seabirds on the U.S. West Coast have yet to be exposed to offshore wind turbines, and their expected behavior when interacting with offshore wind turbines is therefore not well understood.

## 9. References


Adams, J., Kelsey, E.C., Felis, J.J., and Pereksta, D.M., 2017, Collision and displacement vulnerability among marine birds of the California Current System associated with offshore wind energy infrastructure (ver. 1.1, July 2017): U.S. Geological Survey Open-File Report 2016-1154, 116 p., https://doi.org/10.3133/ofr20161154.

H. T. Harvey & Associates, R. G. Ford Consulting Company, NOAA Southwest Fisheries Science Center, Oregon State University, Schatz Energy Research Center. Interim Project Report – (Task 3), Seabirds in 3D: A Framework to Evaluate Collision Vulnerability with Future Offshore Wind Developments.

Ali Jahan, Kevin L. Edwards, Marjan Bahraminasab, Multi-criteria Decision Analysis for Supporting the Selection of Engineering Materials in Product Design (Second Edition),Butterworth-Heinemann, 2016, Pages 63-80, https://www.sciencedirect.com/science/article/pii/B9780081005361000047

Ainley, D. G., E. Porzig, D. Zajanc, and L. B. Spear. 2015. Seabird flight behavior and height in response to altered wind strength and direction. Marine Ornithology 43:25-36.

California State Lands Commission. 2021. “Offshore Wind Applications.” January 25, 2021. https://www.slc.ca.gov/renewable-energy/offshore-wind-applications/.

Carrillo, Victor Manuel, "Development Of New Mathematical Methods For Post-Pareto Optimality" (2012). *Open Access Theses & Dissertations. 1798*.

Collier, Robert, Sanderson Hull, Oluwafemi Sawyerr, Shenshen Li, Manohar Mogadali, Dan Mullen, and Arne Olson. 2019. “California Offshore Wind: Workforce Impacts and Grid Integration.” Center for Labor Research and Education, University of California, Berkeley. https://laborcenter.berkeley.edu/offshore-wind-workforce-grid/.

Fish and Wildlife, Department of the interior. 2011. “Endangered and Threatened Wildlife and Plants; 12-month Finding on a Petition To List the Black-footed Albatross as Endangered or Threatened”. https://www.govinfo.gov/content/pkg/FR-2011-10-07/pdf/2011-25469.pdf#page=1

Leirness, J. B., J. Adams, L. T. Ballance, M. Coyne, J. J. Felis, T. Joyce, D. M. Pereksta et al. 2021. Modeling At-Sea Density of Marine Birds to Support Renewable Energy Planning on the Pacific Outer Continental Shelf of the Contiguous United States. August. OCS Study BOEM 2021-014. Camarillo, California. Prepared for U.S. Department of the Interior, Bureau of Ocean Energy Management, Pacific OCS Region. Prepared by U.S. Department of Commerce, National Oceanic and Atmospheric Administration, and U.S. Department of the Interior, U.S. Geological Survey, Western Ecological Research Center.

Nur, Nadav, Jaime Jahncke, Mark P. Herzog, Julie Howar, K. David Hyrenbach, Jeannette E. Zamon, David G. Ainley, et al. 2011. “Where the Wild Things Are: Predicting Hotspots of Seabird Aggregations in the California Current System.” Ecological Applications 21 (6): 2241–57. https://doi.org/10.1890/10-1460.1.

Pacific Ocean Energy Trust. 2021. “Subsea Transmission Solutions for OSW between CA and OR.” In *POET Webinar Series*. https://pacificoceanenergy.org/2021/04/19/webinar-subsea-transmission-solutions-for-osw-between-california-and-oregon/.

Severy, Mark, Christina Ortega, Charles Chamberlin, and Arne Jacobson. 2020. “Wind Speed Resource and Power Generation Profile Report.” In California North Coast Offshore Wind Studies, edited by Mark Severy, Zach Alva, Greg Chapman, Maia Cheli, Tanya Garcia, Christina Ortega, Nicole Salas, and Amin Younes. Humboldt, CA: Schatz Energy Research Center. schatzcenter.org/pubs/2020-OSW-R2.pdf.

TGS. 2024. “BW-IDEOL Vandenberg Pilot Project Floating Wind Farm” https://www.4coffshore.com/windfarms/united-states/bw-ideol-vandenberg-pilot-project-united-states-us6e.html.

Wallach, E., Carman, J., Alva, Z., Chamberlin, C., and Jacobson, A. “Task 4.1: Offshore Wind Power Generation Scenarios Report.” EPC-19-011. Humboldt, CA: Schatz Energy Research Center.

## Appendix A: Species Included in the 3D Seabird Project

**Table A-1: Name and conservation status of all 44 bird taxa included in the Optimization Framework predictions. ESA-listed refers to species listed as threatened and/or endangered at the federal and/or state level (2 of the 44 taxa) and CSSC refers to species listed as a California Species of Special Concern (4 of the 44 taxa).**

| Latin name | Common name | ESA-listed | CSSC |
|---|---|---|---|
| ***Brachyramphus marmoratus*** | Marbled Murrelet | Yes | No |
| ***Synthliboramphus sp.*** | Scripps's/Guadalupe/Xantus's Murrelet | Yes | No |
| ***Hydrobates homochroa*** | Ashy Storm-petrel | No | Yes |
| ***Hydrobates furcata*** | Fork-tailed Storm-petrel | No | Yes |
| ***Fratercula cirrhata*** | Tufted Puffin | No | Yes |
| ***Ptychoramphus aleuticus*** | Cassin's Auklet | No | Yes |
| *Phoebastria nigripes* | Black-footed Albatross | No | No |
| *Phoebastria immutabilis* | Laysan Albatross | No | No |
| *Fulmarus glacialis* | Northern Fulmar | No | No |
| *Pterodroma cookii* | Cook's Petrel | No | No |
| *Ardenna bulleri* | Buller's Shearwater | No | No |
| *Ardenna creatopus* | Pink-footed Shearwater | No | No |
| *Ardenna griseus* | Sooty Shearwater | No | No |
| *Puffinus tenuirostris* | Short-tailed Shearwater | No | No |
| *Puffinus opisthomelas* | Black-vented Shearwater | No | No |
| *Hydrobates leucorhoa* | Leach's Storm-petrel | No | No |
| *Pelecanus occidentalis* | Brown Pelican | No | No |
| *Phalaropus sp.* | Phalaropes | No | No |
| *Stercorarius longicaudus* | Long-tailed Jaeger | No | No |
| *Stercorarius parasiticus* | Parasitic Jaeger | No | No |
| *Stercorarius pomarinus* | Pomarine Jaeger | No | No |
| *Stercorarius maccormicki* | South Polar Skua | No | No |
| *Larus californicus* | California Gull | No | No |
| *Larus glaucescens* | Glaucous-winged Gull | No | No |
| *Larus heermanni* | Heermann's Gull | No | No |
| *Larus argentatus* | Herring Gull | No | No |
| *Larus occidentalis* | Western Gull | No | No |
| *Larus brachyrhynchus* | Short-billed Gull | No | No |
| *Rissa tridactyla* | Black-legged Kittiwake | No | No |
| *Chroicocephalus philadelphia* | Bonaparte's Gull | No | No |
| *Xema sabini* | Sabine's Gull | No | No |
| *Sterna paradisaea* | Arctic Tern | No | No |
| *Hydroprogne caspia* | Caspian Tern | No | No |
| *Thalasseus elegans* | Elegant Tern | No | No |
| *Urile pencillatus* | Brandt's Cormorant | No | No |

| **Latin name** | Common name | ESA-listed | CSSC |
|---|---|---|---|
| *Nannopterum auritus* | Double-crested Cormorant | No | No |
| *Urile pelagicus* | Pelagic Cormorant | No | No |
| *Uria aalge* | Common Murre | No | No |
| ***Cerorhinca monocerata*** | Rhinoceros Auklet | No | No |
| ***Cepphus columba*** | Pigeon Guillemot | No | No |
| ***Aechmophorus sp.*** | Western or Clark's Grebe sp. | No | No |
| *Gavia immer* | Common Loon | No | Yes |
| ***Gavia pacifica*** | Pacific Loon | No | No |
| ***Gavia stellata*** | Red-throated Loon | No | No |
| ***Melanitta perspicillata*** | Surf Scoter | No | No |